Chapter 5

Sonic Velocity and Other Petrophysical Properties of Source Rocks of Cody, Mowry, Shell Creek, and Thermopolis Shales, Bighorn Basin, Wyoming

Click here to return to
Volume Title Page

By Philip H. Nelson

Chapter 5 of
Petroleum Systems and Geologic Assessment of Oil and Gas in the Bighorn Basin Province, Wyoming and Montana
By U.S. Geological Survey Bighorn Basin Province Assessment Team

U.S. Geological Survey Digital Data Series DDS–69–V

U.S. Department of the Interior
U.S. Geological Survey

U.S. Department of the Interior
KEN SALAZAR, Secretary

U.S. Geological Survey
Marcia K. McNutt, Director

U.S. Geological Survey, Reston, Virginia: 2010

Suggested citation:
Nelson, P.H., 2010, Sonic velocity and other petrophysical properties of source rocks of Cody, Mowry, Shell Creek, and Thermopolis Shales, Bighorn Basin, Wyoming: U.S. Geological Survey Digital Data Series DDS–69–V, 39 p.

ISBN: 1–4113–2667–5

Contents

Figures

Tables

Sonic Velocity and Other Petrophysical Properties of Source Rocks of Cody, Mowry, Shell Creek, and Thermopolis Shales, Bighorn Basin, Wyoming

By Philip H. Nelson

Abstract

The petrophysical properties of four shales are documented from well-log responses in 23 wells in the Bighorn Basin in Wyoming. Depths of the shales examined range from 4,771 to 20,594 ft. The four shales are the Thermopolis (T) Shale, the Shell Creek (SC) Shale, the Mowry (M) Shale, and the lower part of the Cody (C) Shale, all of Cretaceous age. These four shales lie within a 4,000-ft, moderately overpressured, gas-rich vertical interval in which the sonic velocity of most rocks is less than that of an interpolated trendline that reflects a normal increase of velocity with depth. Sonic velocity, resistivity, neutron, caliper, and gamma-ray values were determined from well logs at discrete levels in each of the four shales in 23 wells.

Sonic velocity in all four shales increases with depth to a present-day depth of about 10,000 ft; below this depth sonic velocity remains relatively unchanged. Velocity (V), resistivity (R), neutron porosity (N), and hole diameter (D) from caliper logs in the four shales vary, such that $V_M > V_C > V_{SC} > V_T$, $R_M > R_C > R_{SC} > R_T$, $N_T > N_{SC} \approx N_C > N_M$, and $D_T > D_C \approx D_{SC} > D_M$. These orderings can be partially understood on the basis of rock descriptions. The Mowry Shale is highly siliceous and by inference comparatively low in clay content, resulting in high sonic velocity, high resistivity, low neutron porosity, and minimal borehole enlargement. The Thermopolis Shale, by contrast, is a black fissile shale with very little silt; high clay content causes low velocity, low resistivity, high neutron response, and results in the greatest borehole enlargement. The properties of the Shell Creek and lower Cody Shales are intermediate to the Mowry and Thermopolis Shales.

The sonic velocities of all four shales are less than that of an interpolated trendline that is anchored in shales above and below the interval of moderate overpressure. The reduction in velocity varies among the four shales, such that the amount of offset (O) from the trendline is $O_T > O_{SC} > O_C > O_M$, that is, the velocity in the Mowry Shale is reduced the least and the velocity in the Thermopolis Shale is reduced the most. Velocity reductions are attributed to increases in pore pressure during burial, caused by the generation and retention of gas. A model combining concepts and constraints from burial history, pore pressure increase, and sonic velocity-effective stress relations shows how present-day reduced sonic velocities could have developed during burial as a consequence of loading and pore pressure changes.

Introduction

Shales with organic carbon content in excess of one weight percent, when subjected to sufficient temperatures, are recognized as important sources of oil and gas in sedimentary basins. But the petrophysical properties of shales vary considerably as a result of variations in mineralogy, stress, thermal maturity, and even the generation of hydrocarbons. Attempts to use petrophysical properties to infer a desired parameter, such as pore pressure or thermal maturation, must first take into account the properties of individual shales. Because well logs are generally used to obtain an estimate of recoverable hydrocarbons in pore space, much of the petrophysical literature deals with the properties of reservoir rocks, not source rocks, although this disparity is narrowing as some shales are now proving to be prolific reservoirs as well as source rocks.

Petrophysical properties of shales are controlled by effective stress and rock composition; both factors are important, and both receive attention in this study. As effective stress increases, rocks compact, and the effects of compaction can be observed in well logs as a general increase of sonic velocity and density with depth. Japsen and others (2007) reviewed the petrophysical models that link sonic velocity, porosity, and depth in shales and sandstones; normal pore pressure is assumed. Where pore pressure has been elevated above normal hydrostatic pressure during burial history, effective stress is reduced and sonic velocity is less than that expected from a normal compaction trend. In some geologic settings, the resulting reductions in sonic velocity can be used to estimate pore pressure (Bowers, 1994).

Shales are fine-grained rocks with silt-sized and clay-sized components. Mineralogically, shales consist of varying amounts of quartz, feldspar, carbonate minerals, clay minerals, and organic matter. Size mix and mineralogical composition

are interdependent (an increase in clay mineral fraction results in an increase in clay-size material and a complementary decrease in silt-sized material) and both determine the petrophysical properties. For example, increases in the volume fraction of clay minerals, organic matter, or porosity generally produce decreases in sonic velocity and density but cause increases in neutron porosity. Gamma-ray activity is commonly used to infer the fraction of the clay-sized component, and other petrophysical techniques have evolved to infer shale properties from well-log data (Katahara, 2008). MacQuaker and Jones (2002) examined the connection between petrophysical properties and mudstone characteristics in Upper Jurassic strata in the North Sea, relating the neutron-density response to mudstone composition and grain-size trends. Such studies show that mudstone facies form trends on well-log crossplots, but shale mineralogy or grain-size mix cannot be uniquely resolved from a suite of conventional well-log responses.

The systematic decrease in sonic velocity associated with the occurrence of gas and overpressure has been noted by Surdam and others (1997) in several basins in the Rocky Mountain area, including the Bighorn Basin. The cause of this decrease is currently a topic of some debate in the literature. Surdam and others (1997) attributed it mainly to the presence of gas. In a study of sonic logs in strata of comparable age in the Greater Green River Basin, Gutierrez and others (2006) reported that neither pressure nor the presence of gas could account for the effect on velocity, and attributed the velocity decrease primarily to lithology. This paper addresses the question of the anomalous responses in sonic velocity and other petrophysical properties by (1) summarizing previous work on the mineralogy and organic content of shales, gas shows, and overpressure in the Bighorn Basin; (2) illustrating the suppressed sonic velocity and resistivity logs associated with overpressure and the presence of gas in Cretaceous rocks; (3) documenting the petrophysical responses—sonic velocity, electrical resistivity, density, neutron porosity, gamma-ray activity, and borehole enlargement—of four shales in the Bighorn Basin that are considered to be source rocks; and (4) illustrating how reduced sonic velocity can be maintained during burial and uplift. Primary outcomes of this work are (1) each of the four shales examined here differs from the others in its petrophysical expression and these differences are attributed to differences in composition, and (2) sonic velocity and resistivity in the four shales are less than their expected value based on examination of depth trends. These reductions in sonic velocity and resistivity are believed to be the result of overpressure development and the cessation of increased effective stress during burial and maturation. As a consequence, the present-day petrophysical response of an individual shale results from the combined effects of lithology and effective stress history.

Wells selected for this study are distributed across the southern two-thirds of the Bighorn Basin (fig. 1). Petrophysical properties were drawn from the 23 wells listed in table 1. All 23 wells had satisfactory sonic velocity and gamma-ray logs; however, in some wells, the neutron, density, and gamma-ray logs were not available or were of inadequate quality. The four shales studied in this paper were penetrated by 22 of 23 wells, with one well penetrating two of the four shales.

Geologic Setting

The following descriptions of stratigraphy, mineralogy, organic carbon content, and gas shows and overpressure provide a context for understanding the petrophysical responses of the four shales discussed in this report. The structure of the Bighorn Basin, which is illustrated at the stratigraphic level of interest to us by contours on top of the Cloverly Formation (fig. 1), is discussed by Finn and others (Chapter 3, this CD-ROM), as are the depositional setting, stratigraphy, and other topics relevant to the assessment of the hydrocarbon potential of Cretaceous and Tertiary rocks. Most of the 23 wells used in this study (fig. 1) are incorporated into stratigraphic cross sections by Finn (Chapter 6, this CD-ROM) that display well-to-well stratigraphic correlations, hydrocarbon shows, and production throughout the basin.

Definition of Shale Units

The sonic velocity trendline, which extends from the Claggett Member of the Cody Shale to the upper part of the Cloverly Formation, encompasses the strata of anomalous log character. The four shale formations under study are the Thermopolis, Shell Creek, Mowry, and Cody Shales. An entire formation is generally comprised of shale, siltstone, and sandstone, so it is not desirable to determine petrophysical properties over the entire interval of a formation. Instead, well logs were sampled at discrete points within each shale formation, which were characterized by high gamma-ray values. These locations are referred to as shale units in this report and are selected to be representative of their respective shale formations. For example, the Mowry shale unit refers to the short interval within the Mowry Shale from which values of sonic velocity and other logs were determined. The approximate stratigraphic position of four shale units are shown in figure 2, and are the:

1. lower part of the Cody Shale, above a marker referred to as the “chalk kick,”
2. Mowry Shale, siliceous unit, sometimes referred to as the upper part of the Mowry Shale,
3. Shell Creek Shale as designated by Eicher (1962), sometimes referred to as the lower part of the Mowry Shale, and
4. the upper shale of the Thermopolis Shale from Eicher (1962).

The latter three of these four shale units are within shale formations that are summarized in table 2. Pertinent to our

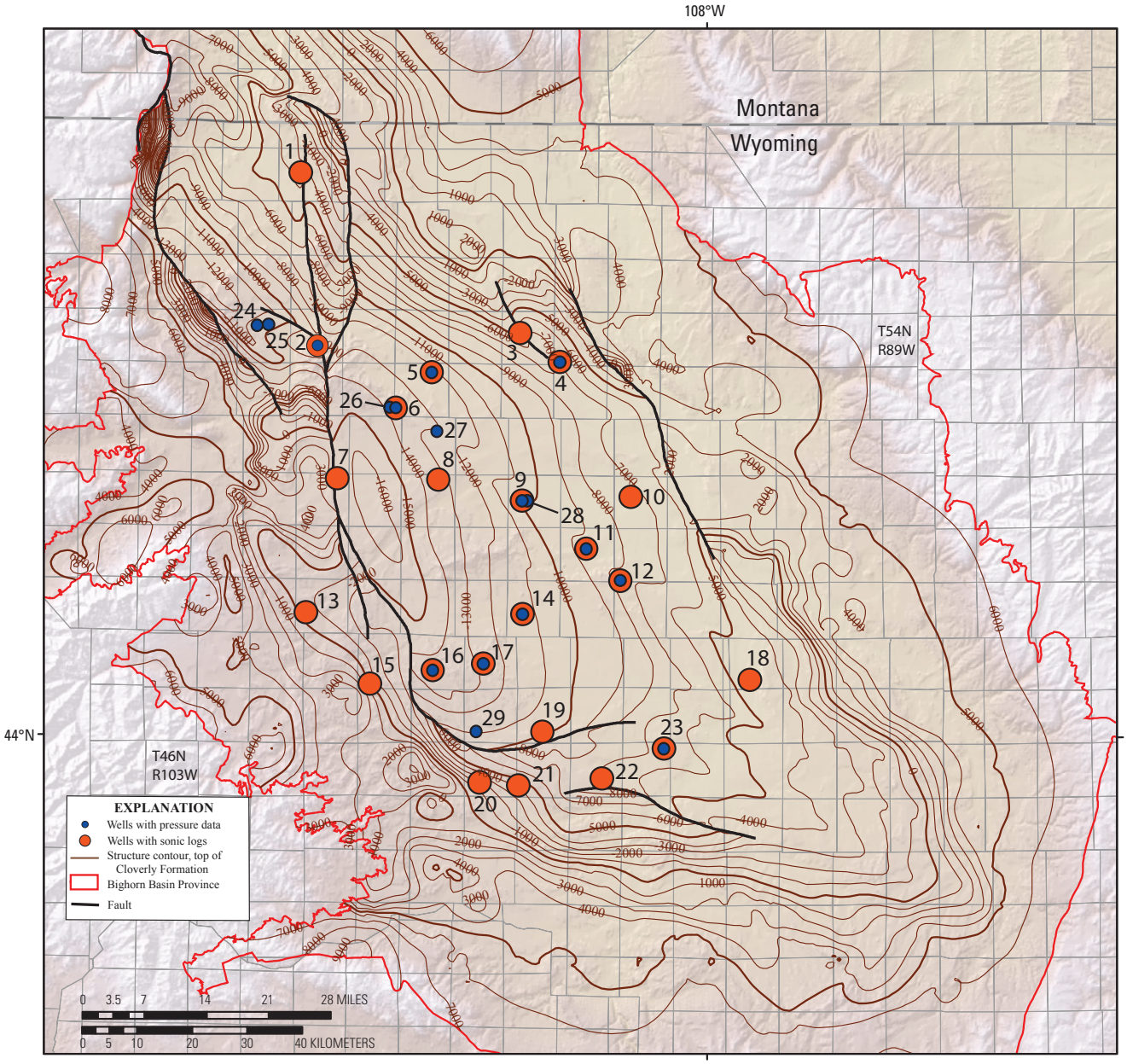

Figure 1. Map of the Bighorn Basin, showing locations of wells used in this study. Wells with sonic logs are listed in table 1 and wells with pressure data are listed in table 5. Structural contours on top of Cloverly Formation from Roberts and others (2008).

Table 1. Location and other information for 23 wells examined for petrophysical responses, Bighorn Basin, Wyoming. First column (No.) is used to identify wells on map in figure 1. All wells penetrated all four shales examined in this report, except the Red Point II Unit well, which did not penetrate the Shell Creek and Thermopolis Shales.

[TD, total depth; API, American Petroleum Institute]

No.	Operator	Lease	Well no.	Section	Township	Range	TD (ft)	API number
1	Excel Energy Corp	State	56-16	16	57N	100W	9,570	49029211050000
2	Amoco Production Co.	McCullough II	3-27	27	54N	100W	13,800	49029209000000
3	Kewanee Oil Co.	Gulch	1	16	54N	96W	12,718	49003201820000
4	True Oil Co.	Spear-Federal	33-31	31	54N	95W	13,380	49003203640000
5	Amoco Production Co.	Bridger Trail Unit	2-A	2	53N	98W	17,060	49029208550000
6	Texas Pacific Oil	Red Point II Unit	1	30	53N	98W	18,500	49029205320000
7	Hunt/Impel	Katrine Loch	1	2	51N	100W	23,990	49029210090000
8	Forest Oil Corp.	Emblem Bench	1	2	51N	98W	18,636	49029210640000
9	Eastern Minerals	Michaels Ranch	17-15	17	51N	96W	16,536	49003203790001
10	Amoco Production Co.	Adams	1	17	51N	94W	11,895	49003205970000
11	Gulf Oil	Fritz-Federal	1-16 2B	16	50N	95W	13,496	49003205720000
12	Gulf Oil	Predicament	1-31-3D	31	50N	94W	14,569	49003205790000
13	Panther Exploration Inc.	Bar TL	2	20	49N	100W	7,325	49029207300000
14	Santa Fe Energy Corp.	Tatman Mtn Federal	1-20	20	49N	96W	16,145	49003205740000
15	Gulf Oil	Buffalo Creek	1	32	48N	99W	8,526	49029206010000
16	American Quasar Petr.	Sellers Draw Unit	1	21	48N	98W	23,081	49029204890000
17	American Quasar Petr.	Ridge Unit	1-21	21	48N	97W	18,286	49043203800000
18	Union Oil of California	Worland Unit	47T-M28	28	48N	92W	10,569	49043202210000
19	BP America	Gillies Draw Unit	1	28	47N	96W	17,333	49043200930000
20	Midwest Oil Corp.	Gywnn Ranch	1	29	46N	97W	9,854	49017060990000
21	Oil Development of Texas	Blue Mesa	1-30	30	46N	96W	10,530	49043202500000
22	Equity Oil Co.	Federal 15-22	1	22	46N	95W	11,948	49043202390000
23	Tipperary Oil and Gas Co.	Federal	1-2	2	46N	94W	13,245	49043204110000

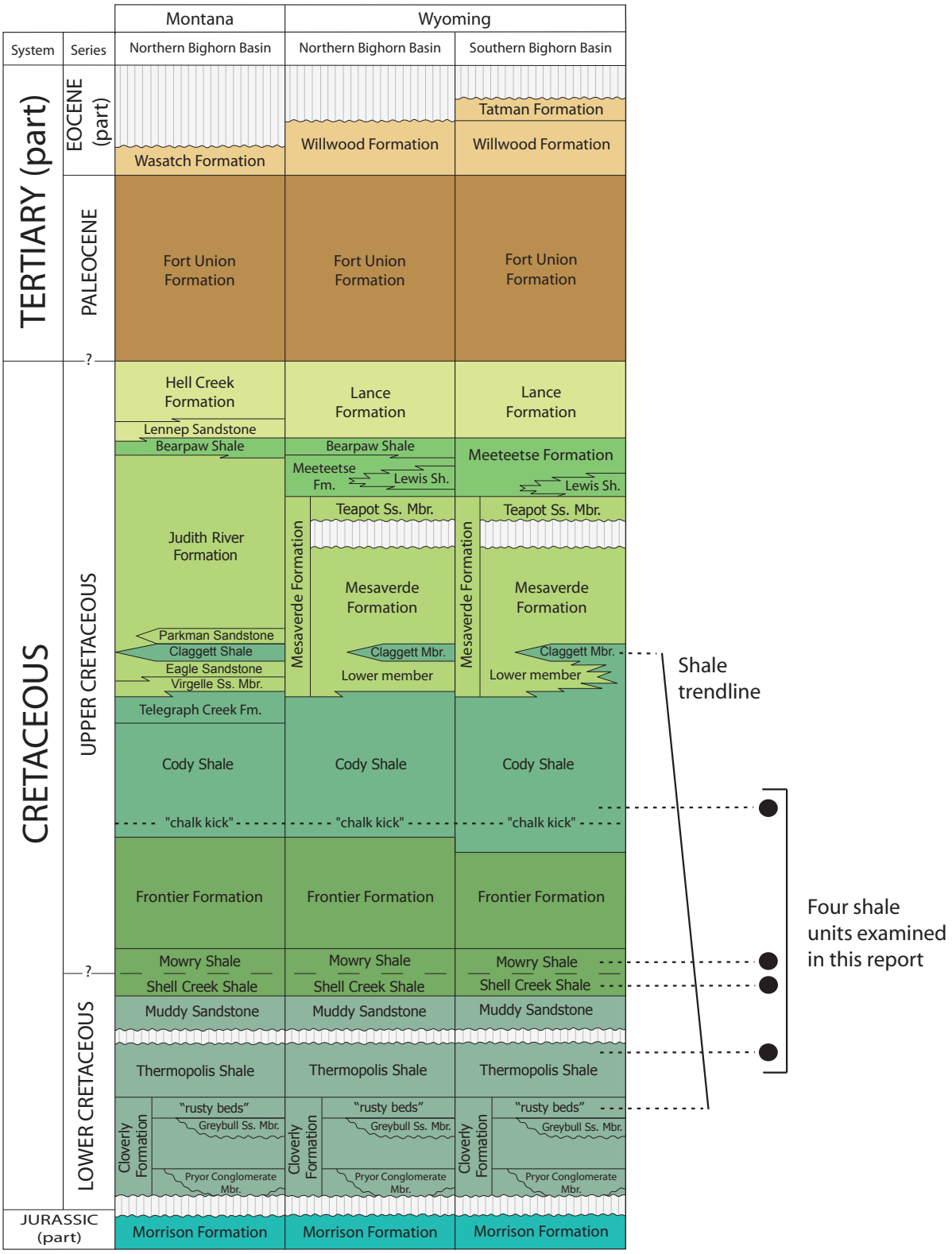

Figure 2. Stratigraphic chart of the Bighorn Basin, Wyoming and Montana, modified from Finn (Chapter 6, this CD-ROM). Black dots and horizontal dotted lines show approximate positions of four shale units where petrophysical values are determined. Shale trendlines are anchored in the Clagget Member of the Cody Shale and the "rusty beds" of the Cloverly Formation.

Table 2. Lithologic descriptions for Mowry, Shell Creek, Thermopolis Shales, and the Muddy Sandstone from Eicher (1962). Petrophysical data analyzed in this report are taken from the Mowry Shale, the Shell Creek Shale, and the upper shale of the Thermopolis Shale.

Rock unit nomenclature of Eicher (1962)	Thickness	Lithologic description	Depositional environment
Mowry Shale (upper part of Mowry according to Keefer and others, 1998).	200 to 300 ft	Consists mainly of dark shale with occasional interbeds of bentonite…shales are extremely hard … because they are composed of a very high proportion of uncombined silica. Unusually resistant.	
Shell Creek Shale (lower part of Mowry according to Keefer and others, 1998).	200 to 300 ft	Dark gray and black shale containing a few ironstone beds …and a few prominent white bentonite beds… some of the shale beds are silty	Continuous deposition in deepening water.
Muddy Sandstone	Generally 30 to 50 ft	Highly variable unit of siltstone, sandstone, shale, and bentonite beds.	A variety of shallow water environments.
Upper shale of Thermopolis Shale.	110 ft in north, 75 ft in south	Fissile black shale which contains very little silt. Contains some ironstone beds and one or two very thin bentonite beds in upper 20 ft.	Deep-water deposition, depleted faunas.
Middle silty shale of Thermopolis Shale.	About 30 ft	Similar to the rusty beds…gray and tan silty shale, thin siltstone and silty limestone beds. More resistant to erosion than the shales above and below.	Possibly shallower water.
Lower shale of Thermopolis Shale.	About 90 ft	Fissile, commonly silty shale that generally contains a few very thin sandstone, ironstone, or sandy limestone beds.	In deeper water than the rusty beds.
Rusty beds of Thermopolis Shale (Cloverly in USGS nomenclature).	About 120 ft	Interlaminated and very thinly interbedded dark shales and gray siltstones…contain much carbonaceous material…also generally contain some brown shale and a few thin beds of ironstone.	Brackish marine water with active currents.

study are the descriptions of the siliceous upper Mowry Shale as being unusually resistant (ridge forming), of the Shell Creek Shale as a dark gray and black shale, and of the upper shale of the Thermopolis Shale as a fissile black shale with little silt. In this paper, the term "Shell Creek Shale" will be used rather than "lower part of the Mowry Shale."

Mineralogy

Studies of shale properties by Ferrell (1962) and Davis (1967, 1970) were based upon x-ray diffraction analysis of outcrop samples. The usefulness of these results to the present study is reduced by the fact that outcrops at the periphery of the basin have never been buried deeper than approximately 5,000 ft, and cannot be expected to represent the mineral assemblages of rocks that had been buried to greater depths. In particular, the conversion of montmorillonite to illite is unlikely to be represented in outcrop samples.

Ferrell (1962) sampled the Thermopolis Shale, Muddy Sandstone, and Shell Creek Shale at three sites on the east flank of the Bighorn Basin. Approximately 105 samples from these sites were analyzed with semi-quantitative x-ray diffraction, meaning that clay minerals could be estimated as a fraction of total clays but not as a fraction of whole-rock mineralogy. As the author's purpose was to interpret the paleoenvironments on the basis of the clay mineralogy, scant attention was paid to the non-clay minerals except to report that "quartz was by far the most abundant non-clay mineral in the samples" and "feldspar and gypsum were present in lesser quantities". X-ray diffraction results for the relative abundances of clays were presented graphically (fig. 4 of Ferrell, 1962), and are summarized in table 3. Ferrell stated that most of the montmorillinite appeared to be derived from volcanic ash.

Davis (1967, 1970) presented the results of x-ray diffraction analyses in tabular and map form, based upon samples from 29 outcrop sites throughout Wyoming, seven of which were on the periphery of the Bighorn Basin. He noted that the dominant facies was a siliceous shale that could be characterized as organic-rich siliceous argillite and silty argillite. His study appears to exclude the Shell Creek Shale, although he does divide the Mowry into upper and lower units, without specifying the criteria for the division. The results of Davis (1970) provide a general description of the mineralogy of the Mowry Shale with a single comment on the Shell Creek Shale (table 3). Davis (1967, p. 25) provided a petrologic summary "representative of this (siliceous) facies along the eastern margin of the Bighorn Basin: fine groundmass, 40–45 percent; organic material, 20–25 percent; quartz silt, 30–35 percent; radiolarian tests, <5 percent; and feldspar(?) silt, <5 percent." Regarding this analysis, he notes that "much excess silica that characterizes this facies and produces its distinctive hardness must be clay-sized, because the amount of quartz silt observed petrographically seems typical of ordinary marine shales". Davis (1967, p. 85) also stated that "siliceous Mowry Shale is permeated with clay-sized quartz which in part is a cement between detrital clay and silt particles."

Total Organic Carbon

Finn and others (Chapter 3, this CD-ROM) examined the available data for total organic carbon. Most of the total organic carbon values for the Mowry and Thermopolis Shales fall between one and two weight percent (fig. 19 of Finn and others, Chapter 3, this CD-ROM), with averages of 1.36 and 1.23 weight percent, respectively, as shown in table 4. Some samples listed as Thermopolis in table 4 are likely to be from the lower Mowry or Shell Creek Shale of Eicher (1962). Rock-Eval data indicate that the gas- or oil-generating potential of these two shales, overall, is generally fair to good, as summarized in table 4. The volume percentage of kerogen can be computed from weight percent of total organic carbon by assuming values for the densities of kerogen and total rock-dry fraction (Vernik and Landis, 1996); the volume percent kerogen is roughly three times the weight-percent organic carbon. Consequently, the average kerogen content is around four volume percent, with typical high and low values of around six and three volume percent, respectively.

Gas Shows and Overpressure

Gas shows in mud returns, gas and oil recoveries in drill-stem tests, and modest overpressure have been reported in a number of wells in the center of the Bighorn Basin by Johnson and Finn (1998), who cited these findings as evidence for a basin-centered gas accumulation. Gas shows and production are also posted on stratigraphic cross sections (Finn, Chapter 6, this CD-ROM). Gas shows are observed in many wells throughout the basin in the Frontier Formation as well as in the Muddy Sandstone, Greybull Sandstone Member of the Cloverly Formation, Cody Shale, and Mowry Shale. Johnson and Finn (1998) outlined an overpressured area of approximately five townships at the base of the Mesaverde Formation and an area of approximately 21 townships in the Frontier Formation. No deep drilling has occurred since their review, so no further compilation regarding the distribution of gas and pressure is offered here. Most indications of overpressure are noted in the Cody Shale, Frontier Formation, Mowry Shale, Muddy Sandstone, and Cloverly Formation (figs. 2, 3). These formations are also the locus of decreases in sonic velocity that are the subject of this investigation.

Indicators of present-day pressures are summarized as the ratio of pressure to depth in units of psi/ft (table 5, fig. 1, fig. 3). Fresh water creates a pressure-depth ratio of 0.433 psi/ft, which is referred to as the hydrostatic gradient. The pressure-depth ratio obtained from drillstem tests is less than 0.4 psi/ft in the Fort Union and Lance Formations, ranges from 0.30 to 0.53 in the Meeteetse and Mesaverde Formations, and, except for outliers of 0.37 and 0.62, ranges from 0.42 to

Table 3. Mineralogy of shale formations from immature outcrop samples along margin of basin. X-ray diffraction results from Davis (1970) and Ferrell (1962) were semi-quantitative, so clay mineralogy was not quantified as a fraction of whole-rock composition.

Formation	Mineralogy	Reference
Cody Shale	No analyses	No reference
Mowry Shale	Quartz content exceeds 50 percent in the Bighorn Basin. Feldspar averages around 5 percent. Quantitative estimates of clay and zeolite minerals could not be obtained. In general, mixed-layer clay is the primary clay constituent in the Mowry Shale; montmorillonite and kaolinite are also present. Illite is a minor component. Zeolites are present, not surprising as the Mowry contains tuffaceous units.	Davis, 1970
Shell Creek Shale	High in montmorillonite. Mixed layer clays are present. Kaolinite and illite absent or present in small amounts.	Ferrell, 1962
Shell Creek Shale	Montmorillonite is dominant in the Shell Creek Shale.	Davis, 1970, p. 494.
Upper part of Thermopolis Shale	High in montmorillonite. Kaolinite and mixed layer clays also present. Illite absent or present in small amounts.	Ferrell, 1962

Table 4. Weight percent of total organic carbon from samples from the Bighorn Basin, compiled by Finn and others (Chapter 3, this CD-ROM) from various sources.

Formation	Range	Average	Generating potential	Gas versus oil
Cody Shale	0.12–5.86	≈1.0	Fair, with excellent potential locally	Mainly a gas-prone source rock
Mowry Shale	0.08–3.6	1.36	Fair to good	Potential to generate oil and gas
Thermopolis Shale	0.37–1.91	1.23	Fair to good	Predominantly gas prone, but has generated oil.

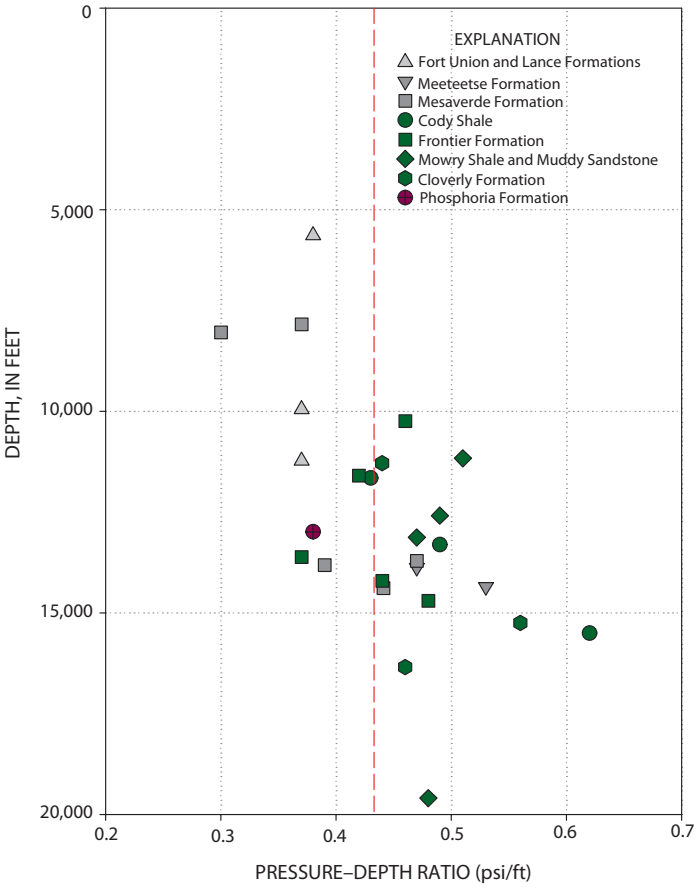

Figure 3. Pressure-depth ratio as a function of depth, from drillstem tests and other sources in the Bighorn Basin. Green symbols designate strata—Cody Shale, Frontier Formation, Mowry Shale and Muddy Sandstone, and Cloverly Formation—where low sonic velocities are commonly observed. Vertical red line shows hydrostatic pressure-depth ratio of 0.433 psi/ft. Values for this graph are taken from table 5.

Table 5. Pressure-depth ratios (PDR, in psi/ft) in wells in the Bighorn Basin, ordered by formation and by depth.Two drillstem tests from the Frontier Formation in CIG McCulloch Peak 1 well were characterized as "near normal" and a value of 0.44 psi/ft was assigned to that interval in this table.

[PDR, pressure-depth ratio; psi, pounds per square inch; DST, drillstem test; wgt, weight; ppg, pounds per gallon; avg, average; JF, data from Johnson and Finn (1998); TP, data from this paper based on IHS Energy (2007)]

No.	Lease	Formation	Average depth (ft)	Method	PDR (psi/ft)	Source
2	McCullough Peak 3-27	Fort Union Fm.(?)	5,639	DST	0.38	TP
26	Stone Barn 14-25	Fort Union Fm.	9,954	DST	0.37	JF
5	Bridger Trail Unit 2-A	Lance Fm.	11,231	DST	0.37	JF
26	Stone Barn 14-25	Meeteetse Fm.	13,877	DST	0.47	JF
6	Red Point Unit 11-1	Meeteetse Fm.	14,354	DST	0.53	JF
12	Predicament	Mesaverde Fm.	7,850	DST	0.37	TP
12	Predicament	Mesaverde Fm.	8,046	DST	0.30	TP
17	Ridge 1-21	Mesaverde Fm.	13,712	DST	0.47	JF
27	Gilmore Hill 1-10	Mesaverde Fm.	13,822	DST	0.39	JF
17	Ridge 1-21	Mesaverde Fm.	14,393	DST	0.44	JF
28	Michael 1-16-4D	Cody (upper)	11,659	DST	0.43	JF
14	Tatman Mountain Federal	Cody Shale	13,307	DST	0.49	TP
6	Red Point Unit 11-1	Cody (upper)	15,500	Mud wgt 12 ppg	0.62	JF
23	Federal 1-2	Frontier Fm.	10,243	DST avg 4 tests	0.46	TP
12	Predicament	Frontier Fm.	11,600	DST	0.42	TP
9	Michaels Ranch 20-1	Frontier Fm.	13,614	DST	0.37	JF
25	CIG McCulloch Peak 1	Frontier Fm.	14,210	DST "near normal"	0.44	JF
24	McCulloch Peak 2-9	Frontier Fm.	14,700	DST	0.48	JF
11	Fritz Federal	Mowry Shale	12,590	DST	0.49	TP
4	Spear Federal	Muddy Sandstone	11,168	DST	0.51	TP
2	McCullough Peak 3-27	Muddy Sandstone	13,129	DST	0.47	TP
16	Sellers Draw	Muddy Sandstone	19,595	Tubing pressure	0.48	JF
23	Federal 1-2	Cloverly Fm.	11,289	DST	0.44	TP
25	CIG McCulloch Peak 1	Cloverly Fm.	15,254	DST	0.56	JF
29	Tenneco 1-29 Federal	Cloverly Fm.	16,347	DST	0.46	JF
4	Spear Federal	Phosphoria Fm.	12,991	DST	0.38	TP

0.56 psi/ft in the Cody Shale, Frontier Formation, Mowry Shale, Muddy Sandstone, and Cloverly Formation. In summary, normal pressure to moderate overpressure is encountered in rocks between the Cody Shale and Cloverly Formation (fig. 3). Together with other considerations, the gas shows and pressure data form the basis for defining the Muddy-Frontier Sandstone and Mowry Fractured Shale Continuous Gas Assessment Unit (fig. 31 of Finn and others, Chapter 3, this CD-ROM). Half of the 23 wells considered in this report lie within this assessment unit.

Modeling of Gas Generation

The generation of oil and gas can alter the stress state and impact the petrophysical response in source rocks, especially the sonic velocity (Vernik and Landis, 1996). Generation of gas and oil was modeled for eight wells in the Bighorn Basin (Roberts and others, 2008); the Tatman Mountain Federal well (location 14 on fig. 1), which is intermediate in terms of burial depths and maximum level of thermal maturity, is used here as a basis for discussion of oil and gas generation in the basin. A summary of oil and gas generation in the Thermopolis Shale in the Tatman Mountain Federal well is shown in figure 4, superposed on the burial history. Gas generation is modeled as beginning at 62 Ma, when the Thermopolis Shale was buried to a depth of 10,000 ft, and ending at 10 Ma, as uplift commences. As indicated in figure 4, oil generation (from Type-II kerogen) commences after the commencement of gas generation (from Type-III kerogen) and peak oil generation occurs soon after peak gas generation. Rapid burial commences around 70 Ma with deposition of the Lance Formation, followed by deposition of the Fort Union and Willwood Formations. The model on which figure 4 is based matches the vitrinite reflectance data in the Tatman Mountain Federal well (fig. 4 of Roberts and others, 2008); measurements show that vitrinite reflectance (R_o) in the Thermopolis Shale is around 1.75 percent, well past the criterion of 0.8 percent that is assumed for peak gas generation from Type-III kerogen.

The Thermopolis and Cody Shales are reported to be predominantly gas-prone and the Mowry Shale to have potential to generate both oil and gas (Finn and others, Chapter 3, this CD-ROM), so the plot of R_o versus depth for Type-III organic matter (fig. 5) pertains to all four shale formations considered in this report. Modeling of hydrocarbon generation from Type-II organic matter, which pertains to the Mowry Shale, and to a lesser extent the Thermopolis Shale, does not account for gas generation directly from kerogen. Thermal maturation was sufficient to generate oil in both the Thermopolis and Mowry Shales, but was insufficient to crack that oil to gas in the Tatman Mountain Federal well (table 5 of Roberts and others, 2008). The relation between thermal maturity as indicated by modeled R_o and depth shows that in most wells an R_o of 0.5 percent is reached at a burial depth of 10,000 to 12,000 ft and an R_o of 0.8 percent is reached at burial depths greater than 15,000 ft (fig. 5). The right-hand depth scale in figure 5 accounts for approximately 5,000 ft of uplift and shows the equivalent present-day depths for which gas generation commenced and reached a maximum. The plot indicates that substantial amounts of gas were generated in rocks that are presently buried 10,000 ft in the center of the basin.

Shale Units and Shale Trendlines Within An Interrupted Compaction Trend

Compaction Trends

As rocks are buried, porosity decreases due to the effects of mechanical compaction and chemical alteration. The decrease in porosity causes gradual decreases in the sonic slowness[1] and, to a lesser extent, increases in the resistivity logs that are manifest as rightward shifts in the logs in the upper 10,000 feet of figures 6*A–D*. The compaction trends are interrupted by leftward excursions of resistivity and sonic logs in the Cody, Mowry, and Thermopolis Shales; the diminished values of resistivity and increased values of sonic slowness within the interval indicated by the orange line and shading in figures 6*A–D* are examined in detail in this paper. Note that the leftward excursions in sonic slowness and resistivity become more clearcut as depth increases (compare the deepest well in fig. 6, Emblem Bench (fig. 6*A*) with the shallowest well, Federal 1–2 (fig. 6*D*)).

Consider the character of the resistivity and sonic logs in the Emblem Bench well (fig. 6*A*). Resistivity increases slightly from an average of 10 ohm-m at 1,000–2,000 ft to an average of 14 ohm-m at 10,100–11,100 ft at the base of the Fort Union Formation. Resistivity ranges from 10 to 100 in the Lance, Meeteetse, and Mesaverde Formations, and the Claggett Member. Resistivity declines from 22 ohm-m at the top of the Cody Shale to a value of 8 ohm-m at the base of the Cody Shale. The lowest values of 4 and 3 ohm-m are reached in the Mowry and Thermopolis Shales. The sonic log has not been edited, so the numerous spikes to the left, with some values exceeding 140 μs/ft, are due to measurement errors sometimes referred to as "cycle skips." Ignoring these sharp leftward spikes, sonic slowness shows a pronounced compaction gradient, decreasing at a fast rate at shallow depth and a slow rate at deeper depth, from greater than 90 μs/ft at

[1]Sonic logs record the time, in microseconds, required for an acoustic wave to travel the distance from source to receiver, in feet. Consequently, the unit of measure is microseconds per ft (μs/ft), variously named transit time, travel time, or slowness. The term slowness is used in this report. High values mean that the acoustic signal is traveling slowly. Well logs are scaled in slowness, but reflection seismologists and laboratory workers use velocity, which is the reciprocal of slowness. Velocity in ft/s is equal to 1,000,000/slowness (μs/ft). For example, a slowness of 80 μs/ft is equivalent to a velocity of 12,500 ft/s. In this paper, slowness is used when examining well logs, and velocity is used when summarizing and comparing results.

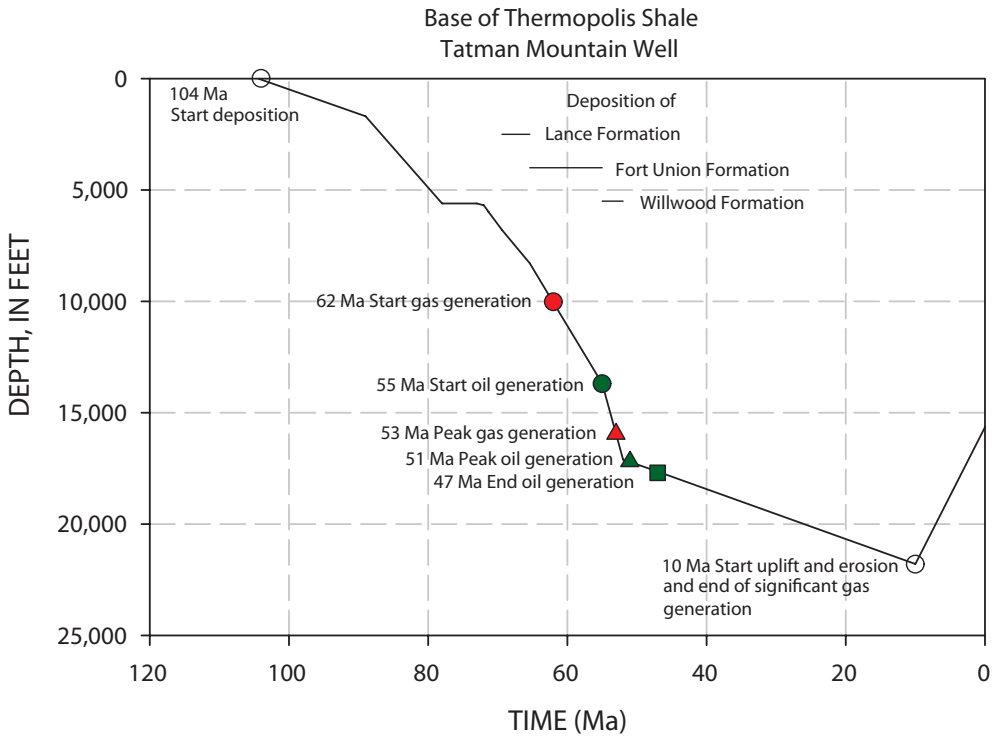

Figure 4. Burial history plot for the base of Thermopolis Shale in the Tatman Mountain Federal well, from Roberts and others (2008), with hydrocarbon generation, depositional, and tectonic events shown as special symbols. Rapid burial of the Thermopolis Shale occurred during deposition of the Lance, Fort Union, and Willwood Formations. Heat flow of 49 mW/m2, constrained by vitrinite reflectance data, and a temperature gradient of 1.30°F/100 ft, based on well data, were used to calculate thermal maturation. The Tatman Mountain Federal well is well 14 in figure 1.

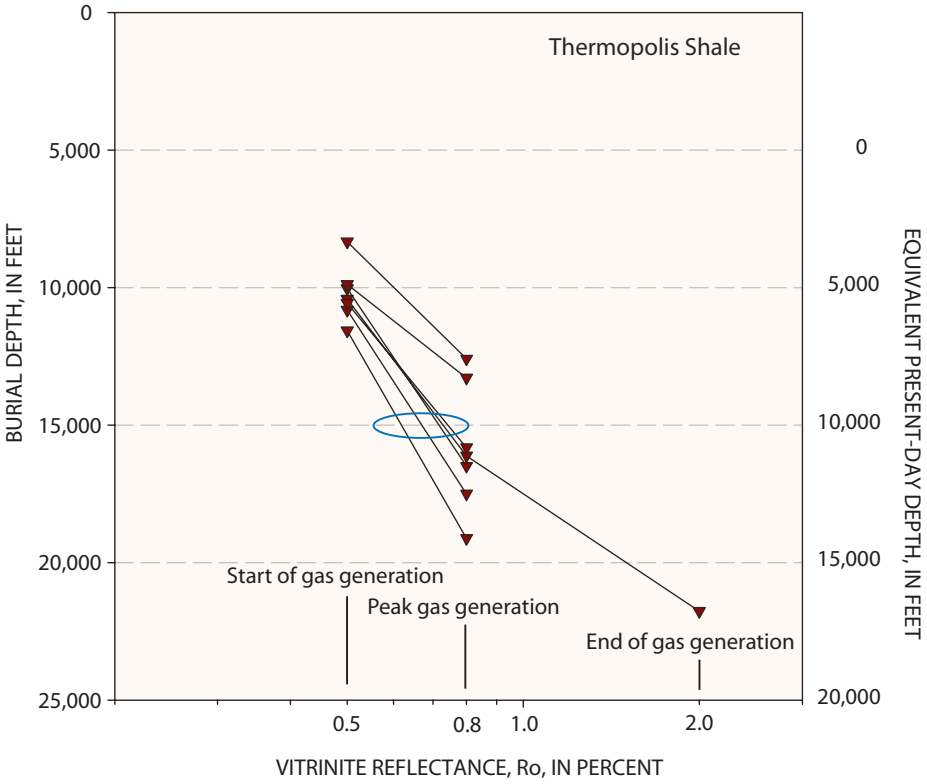

Figure 5. Vitrinite reflectance, computed from one-dimensional burial history models for Type-III source rocks, as a function of burial depth (left scale) and equivalent present-day depth (right scale). Blue ellipse at 10,000 ft present-day depth encloses computational results for the Red Point II, Emblem Bench, Tatman Mountain Federal, Sellers Draw, and McCulloch Peak wells, which are wells 6, 8, 14, 16, and 25–26 respectively in figure 1. From table 4 of Roberts and others (2008).

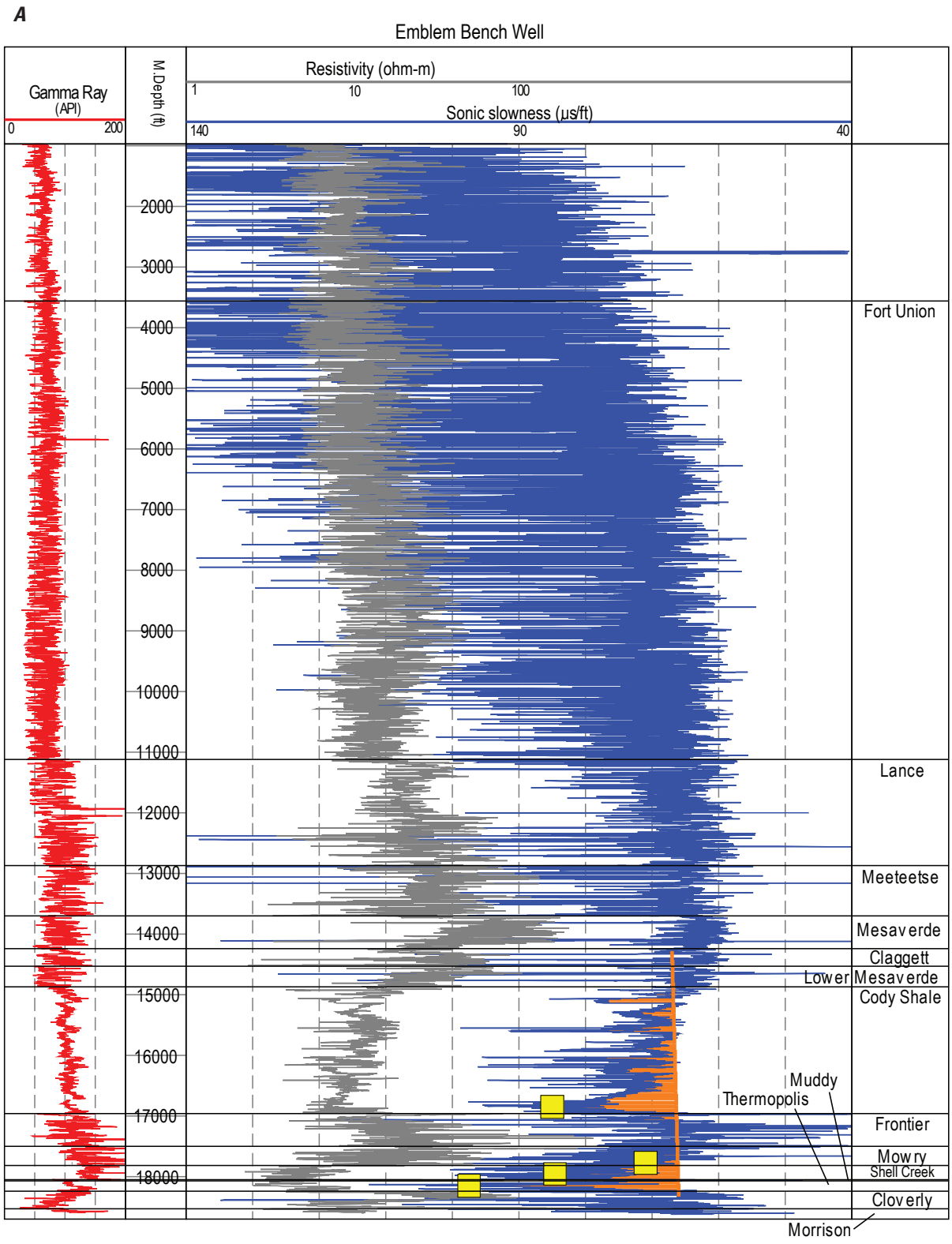

Figure 6 (above, facing page). Gamma-ray, resistivity, and sonic slowness logs in (*A*) Emblem Bench, (*B*) Tatman Mountain Federal, (*C*) Predicament, and (*D*) Federal 1–2 wells. Locations of wells shown in figure 1; well designations are in table 1. Orange line represents the unperturbed sonic slowness in shale, interpolated between an upper point in the Claggett Shale or Mesaverde Formation and a lower point in the Cloverly Formation. Orange shading represents anomalous sonic slowness. Yellow squares are selected sonic slowness values in the Cody, Mowry, Shell Creek, and Thermopolis Shales. Stratigraphic ages of geologic formations are given in figure 2.

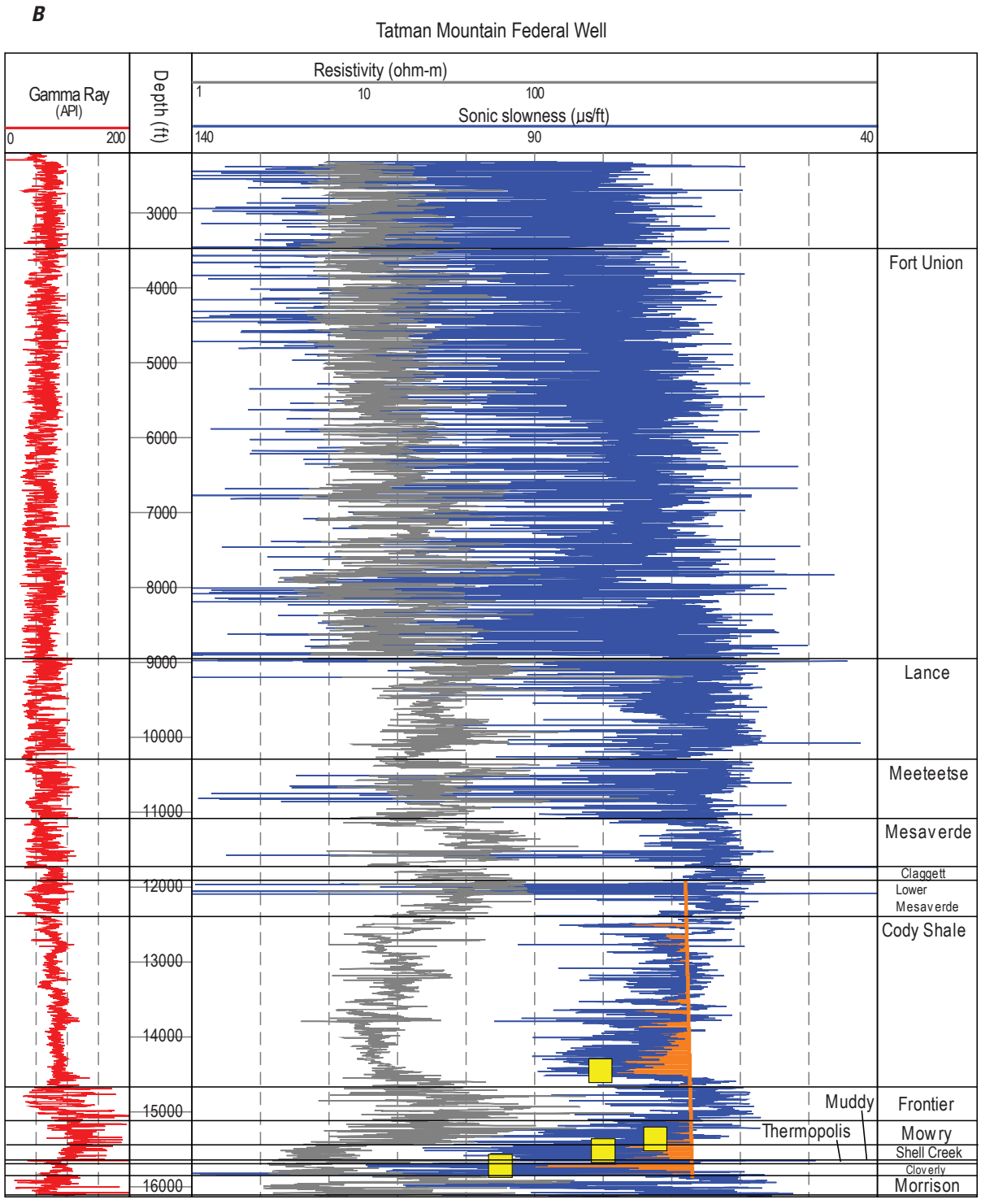

Figure 6.—Continued

C

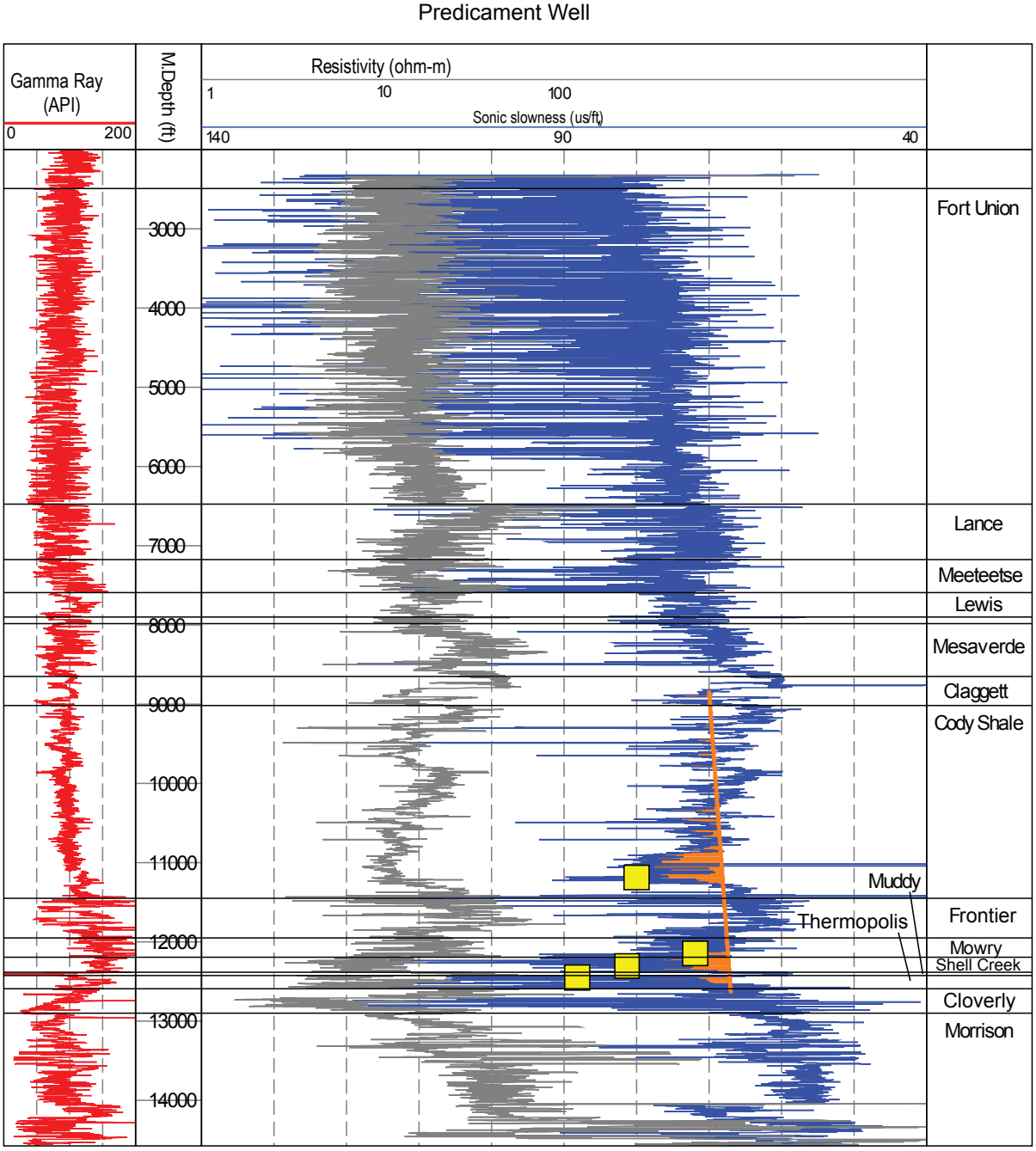

Figure 6.—Continued

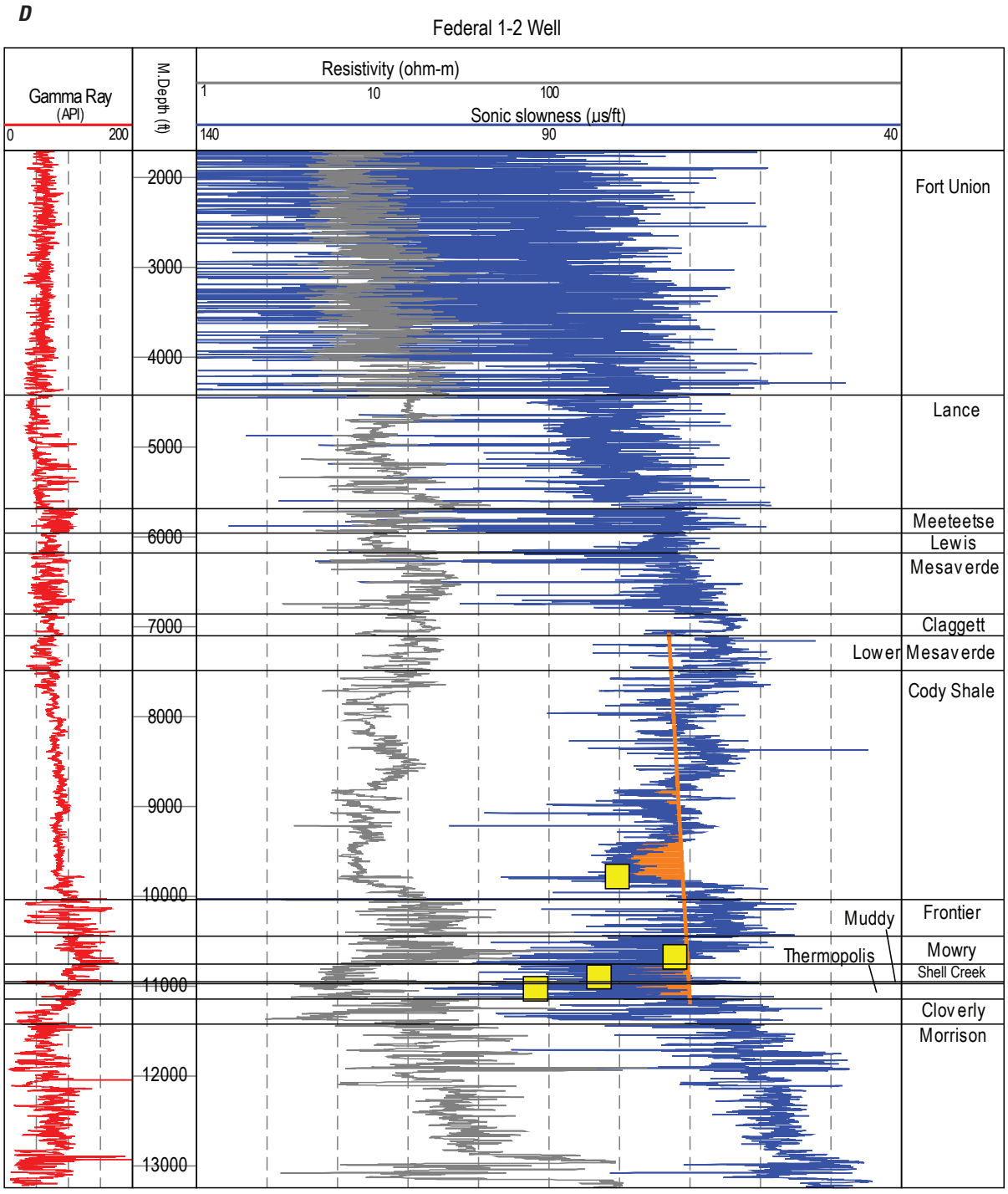

Figure 6.—Continued

depths less than 2,000 ft to a value of 70 µs/ft at the base of the Fort Union Formation. Variations in lithology at the scale of tens and hundreds of feet cause variations in sonic slowness visible as a band of finite width that is particularly visible in the Fort Union and Lance Formations—the left-hand edge of the sonic log represents high gamma-ray or "shaly" rocks and the right-hand edge corresponds to low gamma-ray or "sandy" rocks. Like the resistivity log, the sonic log breaks to the left at the top of the Cody Shale at a depth of 14,860 ft and reaches a value of 85 µs/ft (11,765 ft/s) designated by the yellow square at 16,850 ft at the base of the Cody Shale. High slowness (low velocity) values, also designated by yellow squares, are reached near the base of the Mowry Shale at 17,953 ft (85 µs/ft; 11,765 ft/s) and in the Thermopolis Shale at 18,148 ft (98 µs/ft; 10,200 ft/s). The orange shading indicates the amount of increased slowness (decreased velocity) from an interpolated trendline that represents the expected value of slowness in shales in this interval. There is no unambiguous method to establish such a trendline; the method used in this paper is described below.

Selection of Four Shale Units

The four shale units that are the subject of detailed study in this report are highlighted by yellow squares in figure 7. The value for the lower Cody Shale is taken from a shale unit near the base of the Cody Shale. The sonic slowness of the lower three units, in the Mowry, Shell Creek, and Thermopolis Shales, are also shown on an expanded section in figure 8. The resistivity log provides a clear separation of the Shell Creek and Mowry Shales (fig. 8). The Mowry is more siliceous than the Shell Creek (table 2) and consequently has a lower value of sonic slowness and a higher resistivity than does the Shell Creek. Bentonitic units in the Mowry and Shell Creek Shales characterized by high gamma-ray, low resistivity, and low sonic velocity spikes are avoided in selecting the shale units. The Thermopolis Shale is represented by the sonic slowness of the "upper shale" described by Eicher (1962) in his three-part description of the Thermopolis (fig. 8, table 2) as a fissile black shale. In each well, the shale unit was selected at about the same proportional distance from a top or base of the shale formation, no claim is made that a shale unit is traceable across the basin. From figure 8, it can be seen that variations in resistivity and sonic slowness within a shale formation (Mowry Shale, Shell Creek Shale, and upper shale of Thermopolis Shale) are substantially less than variations among the three formations. As will be seen, the variations of sonic slowness among the lower Cody, Mowry, Shell Creek, and the Thermopolis shale units are consistent from well to well and indicate that a lithologic control on sonic velocity must be taken into account in extracting an overpressure signature from the sonic logs.

Selection of End Points for Shale Trendlines

The two end points defining the shale trendline in the sonic slowness log are placed in the shallowest and deepest "shaly" units that lie above the Cody Shale and below the Thermopolis Shale, and are within rock units deposited in a marine and coastal environment. The upper end point lies in a high gamma-ray unit, placed in the Claggett Shale Member in figure 7, or in the Mesaverde Formation or Cody Shale in other wells. The lower end point lies in a shale in the "rusty beds" of the Cloverly Formation (fig. 8). Shale in the "rusty beds" is characterized by high gamma-ray activity and sonic slowness that is similar to that in the lower part of the Cloverly and the underlying Morrison Formation—thus the shales of the "rusty beds" seem to provide a consistent representation of the normally pressured sequence below the source rocks of the Thermopolis, Mowry, and Cody Shales. Note that sonic slowness in the sandstones of the Cloverly Formation, which are recognized by gamma-ray values less than 50 API units, is less than that of the trendline (fig. 8). Sonic slowness in the siltstones and shales just below the Greybull Sandstone Member (15,960–16,000 ft in fig. 8) is greater than that of the extrapolated shale trendline and may represent an overpressured zone within the Cloverly Formation; this unit was not analyzed in this paper.

Pressure Transition Zone at Base of Cretaceous

As previously stated, the base of the trendline, which is thought to correspond to the base of a pressure compartment, is placed within the Cloverly Formation, although in some wells it could easily have been placed within the Morrison Formation. Rock units deeper than the Morrison Formation are considered normally pressured, based on a variety of measurements from oil and water wells and outcrop (Bredehoeft and others, 1992). The transition from normal pressure in Paleozoic strata to overpressure (or paleo-overpressure) in Cretaceous strata appears to take place within a vertical thickness of several hundred feet in a heterogeneous sequence of mudstone, siltstone, and sandstone. Moberly (1962) noted that "the great bulk of all these formations (Morrison through Mowry) is fine volcanic ash from the Nevadan orogeny that altered under a variety of nonmarine and marine conditions to produce the main stratigraphic units, mudstones and shales." This observation is germane to the nature of the pressure transition zone, because of (1) the predominance of mudstones, claystones, and fine-grained sandstones which are expected to have high capillary entry pressures; and (2) the prevalence of rocks derived in part from volcanic ash, which commonly alters to clay minerals that occlude pores and pore throats, even in shales. Descriptions taken from Moberly (1960, 1962), are cited in table 6 to detail the heterogeneity of the Morrison and Cloverly Formations that play an important role in establishing a pressure transition zone.

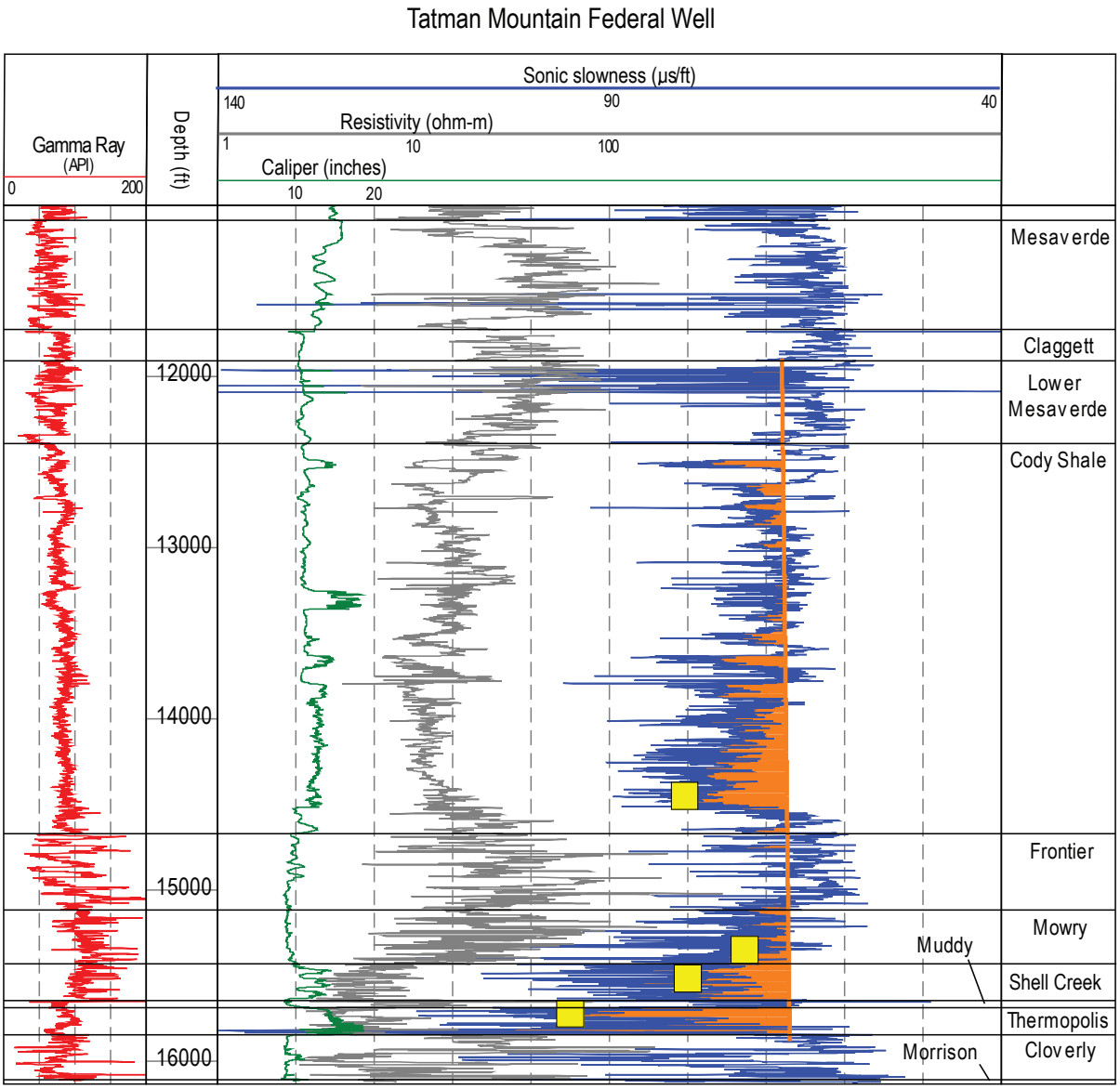

Figure 7. Well logs from the lower 5,000 ft of the Tatman Mountain Federal well, illustrating the selection of the shale trendline and four sonic slowness values, designated by yellow squares, in shale units in the Cody Shale, Mowry Shale, and Thermopolis Shale. Shaded area indicates departure of sonic slowness from a shale trendline.

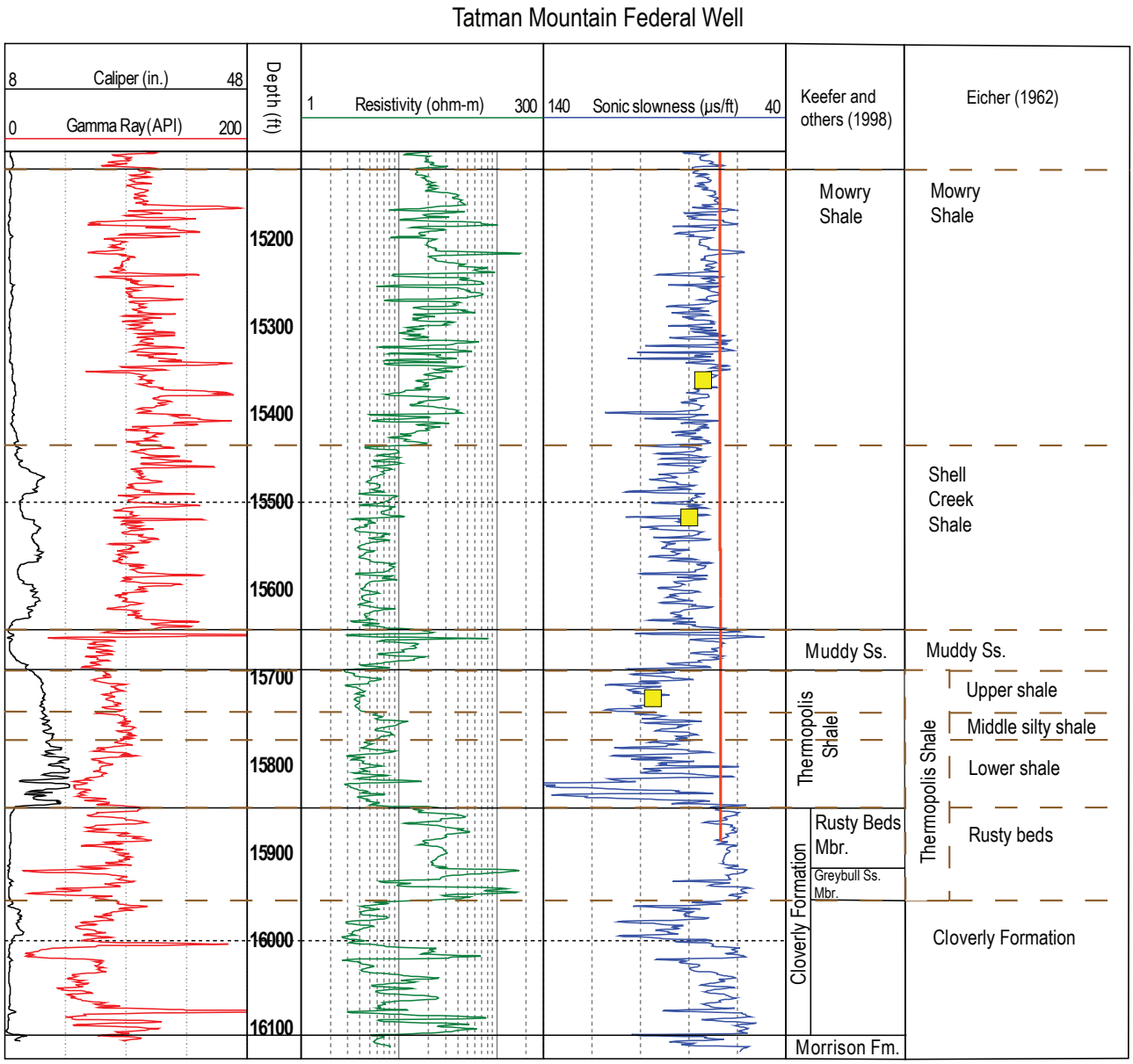

Figure 8. Well logs from the lower 1,000 ft of the Tatman Mountain Federal well, showing lithologic units discussed by Keefer and others (1998) and Eicher (1962). Squares show three sonic slowness values in the Mowry and Thermopolis Shales, vertical orange line is the shale trendline for the sonic log. Lithology descriptions by Eicher (1962) are summarized in table 2.

Table 6. Lithologic description and depositional environment of Morrison, Cloverly, and Sykes Mountain Formations, from Moberly (1960, 1962). The Sykes Mountain Formation of Moberly is included as part of the Cloverly Formation in this paper.

[Mbr, member; Fm., formation]

Rock unit nomenclature of Moberly, 1960	Thickness range and (average), in ft	Lithologic description	Depositional environment
Sykes Mountain Fm.	100– 300 (136)	Rusty weathered ironstone, siltstone, and sandstone, interbedded with thin dark shales. All common clay minerals are present.	Tidal flats and lagoons peripheral to Thermopolis seaway.
Himes Mbr. of Cloverly Fm.	60–120 (92)	Claystone and sandstone channeled with better sorted sandstone; cliff former. (Includes Greybull sandstone of other authors).	Leaching and subaerial weathering of volcanic debris and other sediments.
Little Sheep Mudstone Mbr. of Cloverly Fm.	75–290 (250)	Variegated bentonitic mudstone with some chert pebble sandstone lenses. Bedding is generally absent.	Subaqueous weathering of volcanic debris in lakes and swamps.
Pryor Conglomerate Mbr. of Cloverly Fm.	--	Conglomerate beds or conglomeratic sandstone	--
Morrison Formation	130–280 (190)	Greenish mudstone and sandstone, red-banded in part, with calcareous quartz arenites and subordinate limestones.	Fluvial and lacustrine

Characteristics of Shale Trendlines

Values for the upper and lower end points of trendlines determined for 23 wells are shown in figure 9, where both slowness and velocity scales are shown. Sonic slowness at the upper end of the trendline (Claggett Shale and upper part of the Mesaverde Formation) decreases rapidly with depth to about 8,000 ft and then exhibits only a further slight decrease with increasing depth (fig. 9*A*). Velocity in the Claggett Shale and upper part of the Mesaverde Formation reaches a high value of 15,400 ft/s (65 µs/ft) at 7,500 ft present-day depth (fig 9*A*). Sonic slowness at the lower end of the trendline (Cloverly Formation) undergoes a break in slope around 9,000 to 10,000 ft present-day depth, below this depth range the slowness displays only a further small decrease with increasing depth (fig. 9*B*). The highest velocity of 15,900 ft/s (63 µs/ft) is reached in shaly rocks of the upper Cloverly Formation at 17,000 ft.

These limiting values of sonic slowness are reflected in the near-vertical line segments at 10,000 ft and deeper (fig. 10), where the horizontal scale is sonic velocity rather than sonic slowness as in previous plots. The slopes of the trendlines also show a change at around 10,000 ft (fig. 10). Below 10,000 ft, sonic travel time at the upper end of the trendline is slightly less than at the lower end, giving these trendlines a much steeper slope than those above 10,000 ft. Overall, the line segments reflect shale compaction as a function of depth in the Bighorn Basin; the line segments at depths less than 10,000 ft have lower velocities and smaller slopes than the line segments at depths greater than 10,000 ft. Compaction appears to have greatly diminished below present-day depths of 10,000 ft.

Petrophysical Properties of Four Shale Units

The values of five petrophysical properties—sonic velocity, electrical resistivity, density, neutron porosity, and gamma-ray activity—were determined from well logs for the four shale units. The caliper reading was also noted as an indicator of the tendency for the borehole wall to slough. Wells were drilled and logged by Schlumberger and Dresser Atlas between 1972 and 1982 with the exception of the Gywnn Ranch well, which was drilled in 1965. Values and statistics for each shale unit are tabulated in Appendix 1.

Shales tend to wash out when drilled, resulting in a borehole diameter that is greater than the bit diameter. The interval of the Tatman Mountain Federal well shown in figure 7 was drilled with a bit diameter of 8.5 in. but the hole diameter is greater than 10 in. throughout much of the interval and exceeds 14 in. in the Thermopolis Shale. The borehole diameter in each of the shale intervals was tabulated (Appendix 1) and subtracted from the bit size. Borehole enlargement ranges from about 1 to 9 in. in the lower Cody, Shell Creek, and Thermopolis shale units, is generally greatest in the Thermopolis shale unit, and is generally less than 2 in. in the Mowry shale unit (fig. 11). All wells were drilled with

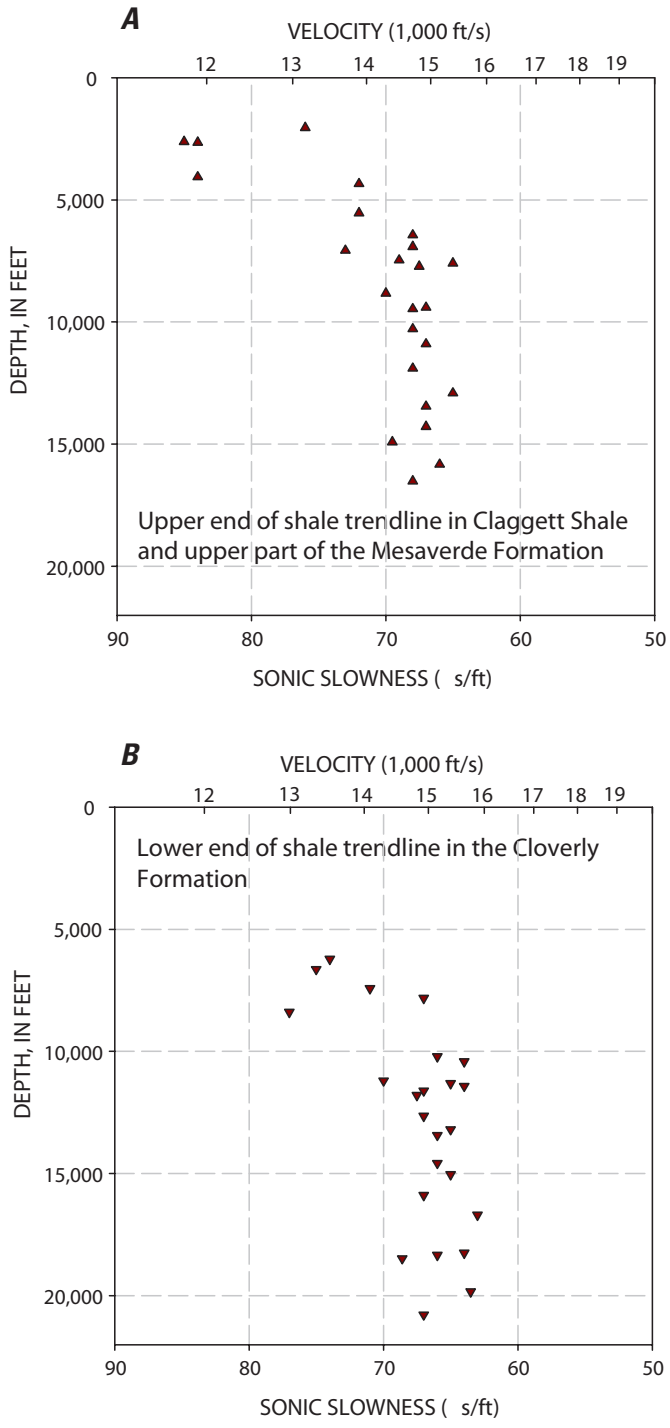

Figure 9. Sonic slowness as a function of depth in 23 wells. *A*, Value selected in Claggett Shale for upper end of shale trendline, and *B*, value selected in Cloverly Formation for lower end of shale trendline.

water-based muds, except for the Gywnn Ranch well which was drilled with an oil emulsion, and the Katrine Loch well which was drilled with an oil-base mud (Appendix 1). As a consequence of drilling with an oil-base mud, the borehole diameter in the Katrine Loch well was close to bit size for the entire drilled interval and there was no borehole enlargement in the four shale units (fig. 11). Log properties from the shale units in the Katrine Loch well should be unperturbed by borehole effects. None of the four shale units show any consistent trend of borehole enlargement with depth (fig. 11).

The distinction between transport and bulk properties is useful in considering petrophysical responses. Sonic velocity and resistivity are called transport properties because energy is propagating through the rock and the values of these properties depends upon direction of propagation. Neutron porosity, density, and gamma-ray activity are bulk properties and their determination is insensitive to the mode or direction of energy propagation. The two transport properties are presented first, followed by the three bulk properties.

Sonic velocity was determined with the borehole-compensated sonic log, which measures the travel time of the compressional wave between two receivers spaced 3 and 5 ft from the transmitter. The combined effect of borehole enlargement and formation damage could potentially cause erroneous velocity determinations in shales. If the formation is damaged, as it can be when water in the borehole causes clay minerals to expand, then there is a concern that the sonic log measures the reduced velocity of the altered shale close to the borehole rather than the velocity of the unaltered shale. Indeed, the depth of investigation of a sonic log is quite limited for the case where the velocity of rock next to the borehole is greater than that of the unperturbed formation, but it is not so limited for the case of reduced velocity next to the borehole (Baker, 1984), which corresponds to the situation examined here. An algorithm based on ray-path theory (Appendix B of Baker, 1984), can be used to calculate the minimum thickness of an altered zone required to produce an erroneous result. For example, if the true formation velocity is 14,000 ft/s and the altered zone velocity is 13,000 ft/s, then the sonic log will yield the correct velocity of 14,000 ft/s unless the altered zone is greater than 4 in. thick. It seems unlikely that the thickness of an altered shale layer extends more than 4 in., due to low permeability of shales. Two pieces of field evidence also indicate minimal errors in measuring the formation velocity. The Katrine Loch well was drilled with oil-base mud rather than the water-base mud used in most other wells, which results in a borehole with little enlargement (fig. 11) and no water in contact with shale, so that clay swelling is checked. The sonic velocities determined in four shale units in the Katrine Loch well are close to average values for all wells (Appendix 1 and fig. 10), rather than being the highest of all values as would be the case if all other logs were adversely affected by altered shale. Further inspection found no interdependence between sonic velocity and borehole enlargement in the shale units, as indicated by the summary displayed in table 7. Thus both a theoretical model pertinent to formation alteration and

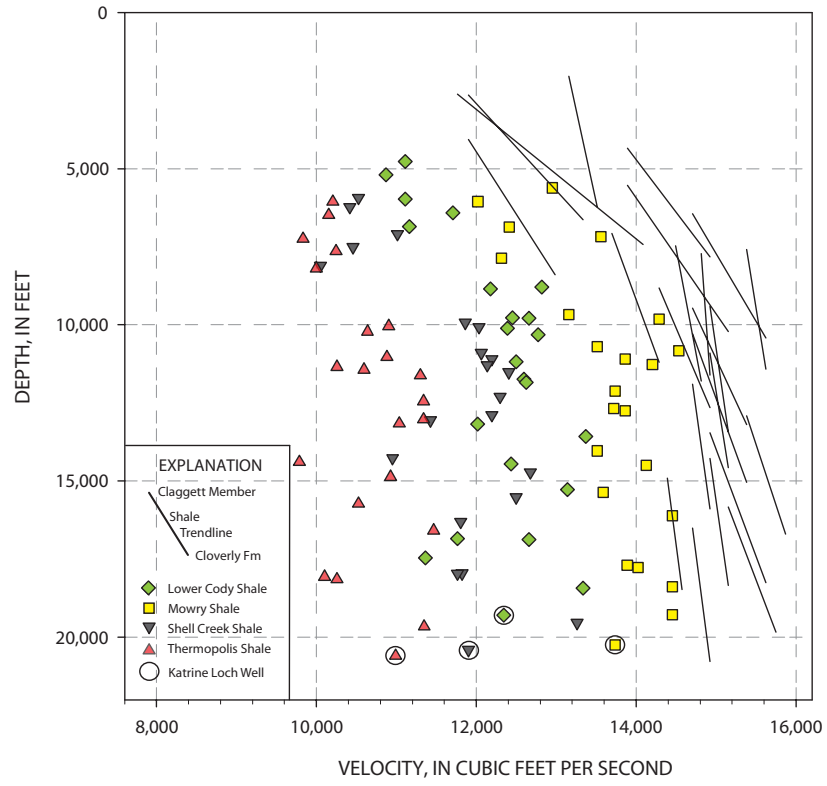

Figure 10. Sonic velocities in four shale units, with shale trendlines, as a function of depth for 23 wells in the Bighorn Basin. Four encircled data are from the Katrine Loch well, which was drilled with oil-base mud. The shale trendlines represent unperturbed velocity trends, as depicted in figures 6 A–D.

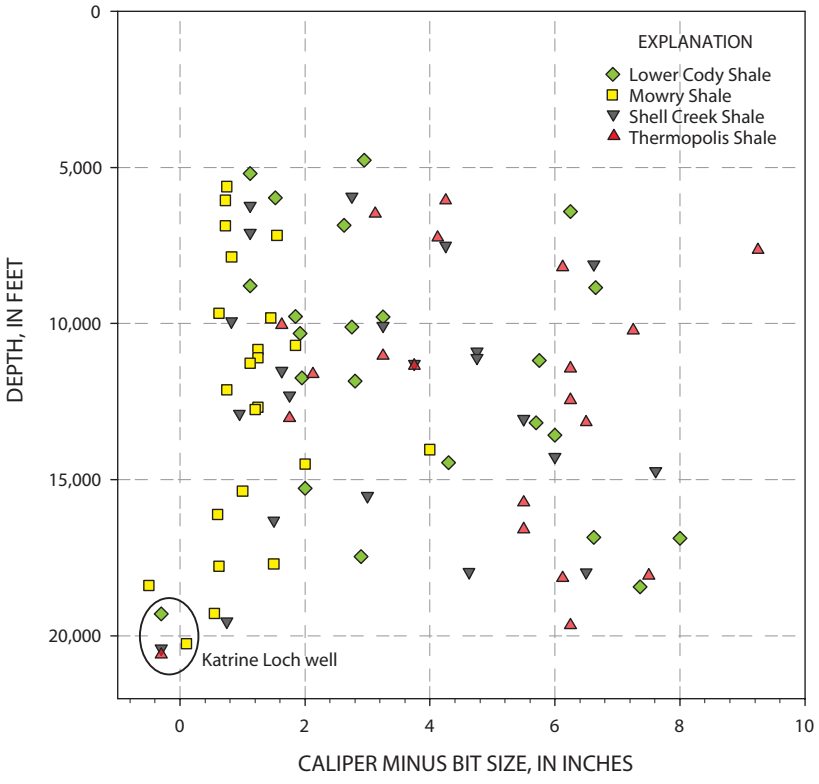

Figure 11. Borehole enlargement in four shale units as a function of depth. The Katrine Loch well was drilled with an oil-base mud.

Table 7. Average values of sonic velocity as a function of borehole enlargement, as determined by the difference between caliper and bit size, for three shale units. Because there was little borehole enlargement in the Mowry shale unit, it is not included in this table.

Shale Unit	Average Sonic Velocity in ft/s	
	Caliper Minus Bit Size < 5 inches	Caliper Minus Bit Size > 5 inches
Lower Cody	12,124	12,442
Shell Creek	11,818	11,374
Thermopolis	10,651	10,687

practical examples incorporating the effects of both borehole enlargement and formation alteration indicate that errors in sonic velocity determination are minimal in the four shale units.

Velocities in the lower Cody, Mowry, Shell Creek, and Thermopolis shale units from 23 wells are plotted with the trendlines in figure 10. The increasing velocities with depth for each of the shales form a trend that generally tracks the overall pattern of the trendlines, for which the increase in velocity with depth lessens at present-day depths greater than 10,000 ft. Separation between the shale velocities and the trendlines is proportional to the orange shading patterns of figure 6. Velocities of the Thermopolis shale unit are systematically less than for the other shales, and velocities of the Mowry shale unit are consistently greater. For depths greater than 8,790 ft (18 wells), the average velocities for the four shale units are: lower Cody, 12,528 ft/s; Mowry, 13,943 ft/s; Shell Creek, 12,083 ft/s; and Thermopolis, 10,826 ft/s. The average velocity in the black, fissile Thermopolis shale unit is 3,117 ft/s less than in the siliceous Mowry shale unit.

Resistivity was determined with the deep laterolog tool in 11 wells and with the deep induction tool in 12 wells. Corrections to the deep laterolog are less than 10 percent for conditions encountered in these wells (Schlumberger, 1996). Corrections to the deep induction log can be greater than 10 percent due to electrical signals generated in conductive mud. The correction depends upon standoff (separation of the tool from the borehole wall), but standoff is difficult to determine. Plots of resistivity with depth showed that resistivity values from the deep laterolog and the deep induction log were intermingled with no offset, indicating that any need for corrections was minor, so no corrections were applied to either the deep laterolog or the deep induction logs. As was apparent in the plot of sonic velocity with depth (fig. 10), resistivity in the shale units increases with depth to depths of around 10,000 ft (fig. 12). However, below the depth range 10,000–12,000 ft, resistivity decreases with depth rather than remaining constant, as was the case for sonic velocity.

Some of the borehole factors that affect the neutron response[2] (Schlumberger, 1996)—mudcake thickness, borehole salinity, formation water salinity, and mud weight—have little impact in the wells studied here. A correction for borehole enlargement was made at the time of logging, as automatic compensation was applied to most neutron logs. But three other factors—tool standoff, temperature, and pressure—do affect the neutron response although no correction has been applied here. A tool standoff of 1 in. from the borehole wall requires a correction of -2 to -3 percent, but this correction is difficult to apply due to lack of a measurement of standoff. For depths ranging from 7,000 to 20,000 ft, the correction for pressure ranges from -0.7 to -2 percent. Bottom-hole temperatures ranging from 140°F to 250°F require neutron porosity corrections ranging from +4 to +9 percent. Given that these three corrections are of opposite sign and somewhat compensating and given the uncertainty involved in applying the corrections, the neutron response values have not been corrected for use in this study. The tabulated neutron response values (Appendix 1) do not show any depth dependence and therefore no depth plot is shown. From Appendix 1, the averages and standard deviations for all samples from all depths are in percent porosity: lower Cody 27, 4; Mowry 18, 2; Shell Creek 30, 7; and Thermopolis 38, 8. The Mowry shale unit has the lowest neutron porosity and the lowest standard deviation of the four shale units, and the Thermopolis shale unit, the greatest.

The density log can produce erroneously low density values if the borehole is not smooth. In the Mowry Shale, the caliper log consistently showed a smooth borehole and the density log had very little correction, but in the other three shale formations, the density correction generally exceeded 0.1 g/cc and the caliper log indicated an enlarged rough borehole (figs. 7 and 11). For this reason, density values are shown for the Mowry shale unit but not for the lower Cody, Shell Creek, or Thermopolis shale units (fig. 13). The density values at depths less than 10,000 ft are less than values at depths greater than 10,000 ft; this increase of density with depth, which is similar to the velocity-depth relation for the Mowry in figure 10, is attributed to compaction. The deepest well in the study, Katrine Loch, was drilled with an oil-base mud instead of a water-base mud, thereby preserving a smooth borehole that is not much greater than bit size. Consequently, valid density data were obtained for all four shale units in the Katrine Loch well: Thermopolis, 20,594 ft, 2.65 g/cc; Shell Creek, 20,399 ft, 2.67 g/cc; Mowry, 20,246 ft, 2.63 g/cc; and lower Cody, 19,926 ft, 2.64 g/cc. Thus, at high levels of effective stress in the deep Katrine Loch well, the density values of the four shale units are similar at 2.65±0.02 g/cc.

[2]The neutron log responds primarily to hydrogen concentration. Most of the hydrogen present in rocks is in water and hydrocarbons, so a neutron log responds to the fluid in the pore space and the term "neutron porosity" is applicable for porous rocks with little clay content. However, because most clay minerals contain substantial amounts of hydroxyls or bound water, the "neutron porosity" response is much greater than actual porosity in siltstones and shales. The neutron porosity values shown in this paper can be considered to be responding primarily to clay content, with only a minor contribution from porosity.

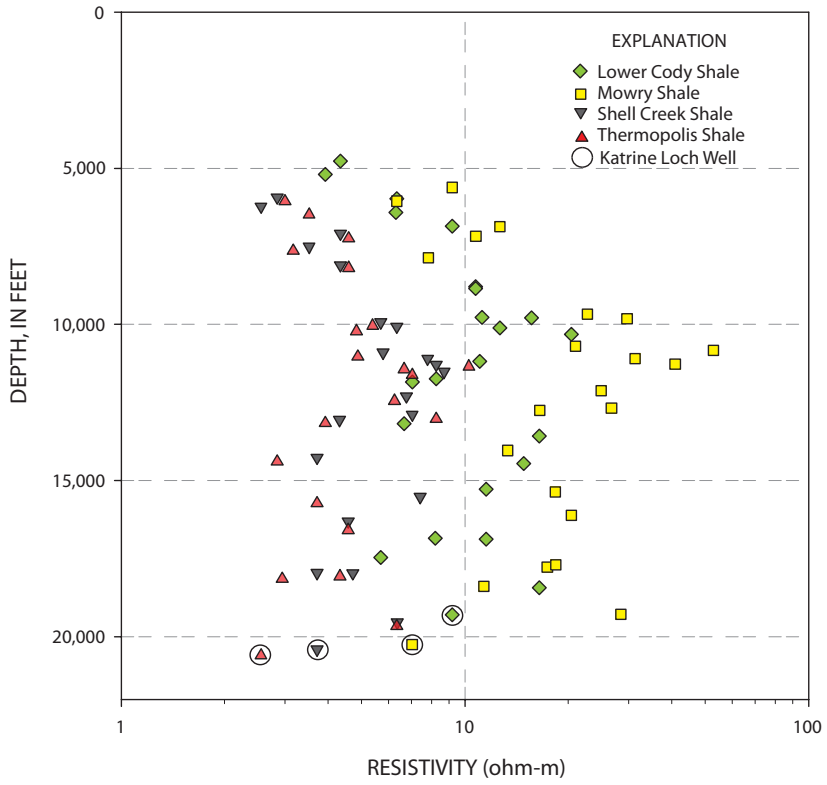

Figure 12. Resistivity for four shale units as a function of depth. Resistivity appears to reach maximum values at depths of 10,000 to 12,000 ft. Four encircled points are from the Katrine Loch well, drilled with oil-base mud.

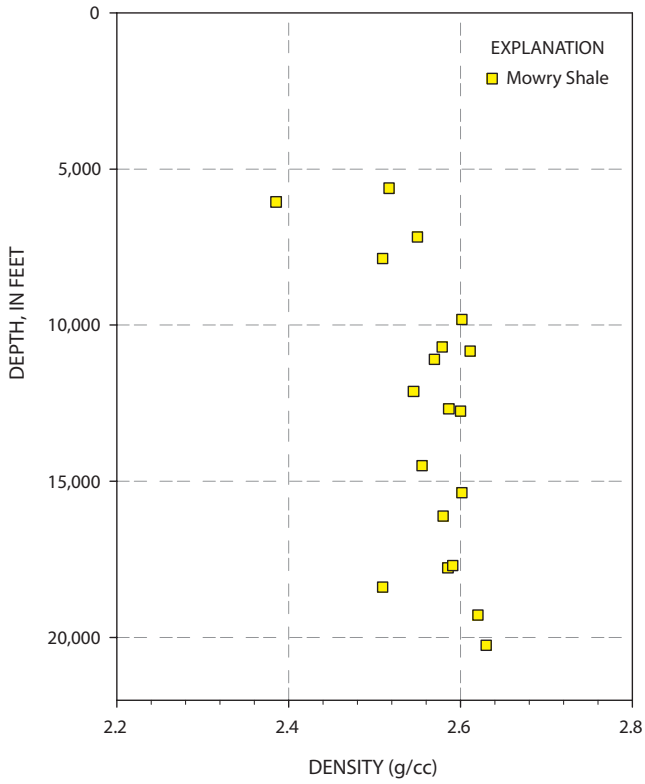

Figure 13. Density for the Mowry shale unit as a function of depth. A compaction effect is evident.

Corrections to the gamma-ray log are needed to account for gamma-ray attenuation in the borehole if a heavy mud is used and the borehole is greatly enlarged. Mud weights used in the wells considered here ranged from 8.8 to 10.7 pounds per gallon (Appendix 1) and enlargement of borehole diameter, as previously discussed, ranged from 0 to 9 in. Using guidelines from Schlumberger (1996) it was found that corrections for gamma-ray attenuation were generally less than 10 percent, so no corrections were applied. One well (Fritz-Federal 1–16 2B, location 11 in fig. 1) was drilled with potassium-chloride mud and exhibited an unusually high gamma-ray response in all shale units, so the gamma-ray values for this well were dropped from the data set. Gamma-ray responses show no dependence upon depth, but there is a dependence upon shale unit as discussed below.

To examine the relationships among petrophysical responses, the values of resistivity, density, neutron porosity, and gamma-ray activity are plotted against sonic velocity (fig. 14). To reduce the effect of compaction, five wells were excluded from the plots, so that no values are shown from depths shallower than 8,750 ft. Sonic velocity is positively correlated with resistivity, with both velocity and resistivity values lowest in the Thermopolis Shale and highest in the Mowry Shale (fig. 14*A*). Density values are available only for the Mowry Shale, where there is no clear relation between sonic velocity and density (fig. 14*B*). Sonic velocity is negatively correlated with neutron porosity (fig. 14*C*). Velocity is highest and neutron porosity is lowest in the Mowry Shale, whereas velocity is lowest and neutron porosity is highest in the Thermopolis Shale. Sonic velocity tends to increase with increasing values of gamma-ray activity (fig. 14*D*), a rather unexpected result because high gamma-ray activity is usually an indicator of shalier, hence mechanically weaker, rocks. Possible causes of these relations will be discussed below.

Neutron-density plots, a common tool of petrophysical analysis, provide a way of evaluating the degree of shaliness in siliciclastic sequences (Katahara, 2008). The neutron and density values of the Mowry shale unit are tightly clustered on the neutron-density plot (fig.15). The sandstone line represents a zero clay line. To show the utility (and limitations) of a neutron-density plot, a modified illite point forms one corner of a skewed three-component triangular diagram that is superposed on the neutron-density coordinates (fig.15). The modified illite point has a neutron porosity of 34.4 percent, as given by Ellis and Singer (2008), and a density of 2.60 g/cc which is greater than their computed value of 2.52 g/cc. Three parallel lines show the illite fraction and the two long sides of the triangle indicate porosity bounds of zero and 10 percent. This diagram indicates that the illite content in the Mowry shale unit ranges from 30 to 55 percent. There is no assurance that this shale unit consists of only pore space, quartz, and illite, so the triangular diagram with a single illite clay point is only an idealization of the true mineralogy. According to the semi-quantitative analyses of Mowry Shale outcrop samples (table 3), mixed-layer clay is the primary clay constituent, with montmorillonite present and illite a minor constituent. It is quite possible that conversion of montmorillonite to illite has increased the illite content of rocks in the deep subsurface that are represented in figure 15. Quantitative mineralogic analysis on samples from deep wells is required to substantiate or improve the interpretation of figure 15.

A statistical summary of the six petrophysical responses (fig. 16) is restricted to depths greater than 8,750 ft to eliminate data points that have not reached the maximum compaction state. The box-and-whiskers summary shows the following order for sonic velocity and resistivity responses:

Mowry > lower Cody > Shell Creek > Thermopolis

This order is reversed for the neutron porosity response. This systematic ordering in four of five petrophysical responses (ordering for the gamma-ray log differs from the others) is related to mineral composition, as discussed next.

Discussion

The petrophysical responses documented thus far are controlled by shale composition and stress history. Petrophysical responses are represented schematically by four horizontal bars showing the range of sonic velocity for depths greater than 8,750 ft in figure 17, along with the range of expected (trendline) velocities for depths greater than 10,000 ft (gray box in fig. 17). To a first approximation, the effect of rock composition is manifested by the variation in velocity among the four shale units, and the effect of stress history is manifested by the reduction of velocity below the range of expected velocities, that is, by the leftward displacement of the four horizontal bars from the gray box. The elements of composition—mineral content, porosity, fluids, and kerogen content—and the manifestations of stress history—overpressure and microfracturing—are summarized in the lower part of figure 17, which serves as a guide for the following discussion.

The mineralogy of shales can vary considerably. Pettijohn (1975) stated that the clay mineral content of shale varies from 40 to 100 percent, although most shales have a large silt fraction comprised of detrital quartz and lesser amounts of feldspar. Kerogen is another common constituent. The estimation of a petrophysical quantity such as sonic velocity from rock composition represents a central activity of experimental and theoretical petrophysics (Hearst and others, 2000, chapters 1 and 12). For example, the dependence of the sonic velocity of siliciclastics upon porosity and clay content has been examined by Vernik (1997); shales are presented as a high-clay end member of a siliciclastic sequence. An increase in the volume fraction of clay minerals and kerogen, both being low modulus (soft) materials, results in lower sonic velocity. Conversely, an increase in silica or carbonate, whether present as grains or cementing material, is expected to increase sonic velocity (arrows in fig. 17). Without mineralogical analyses of samples that correspond to the well-log data, these relations cannot be quantified in this report, but some observations can be made:

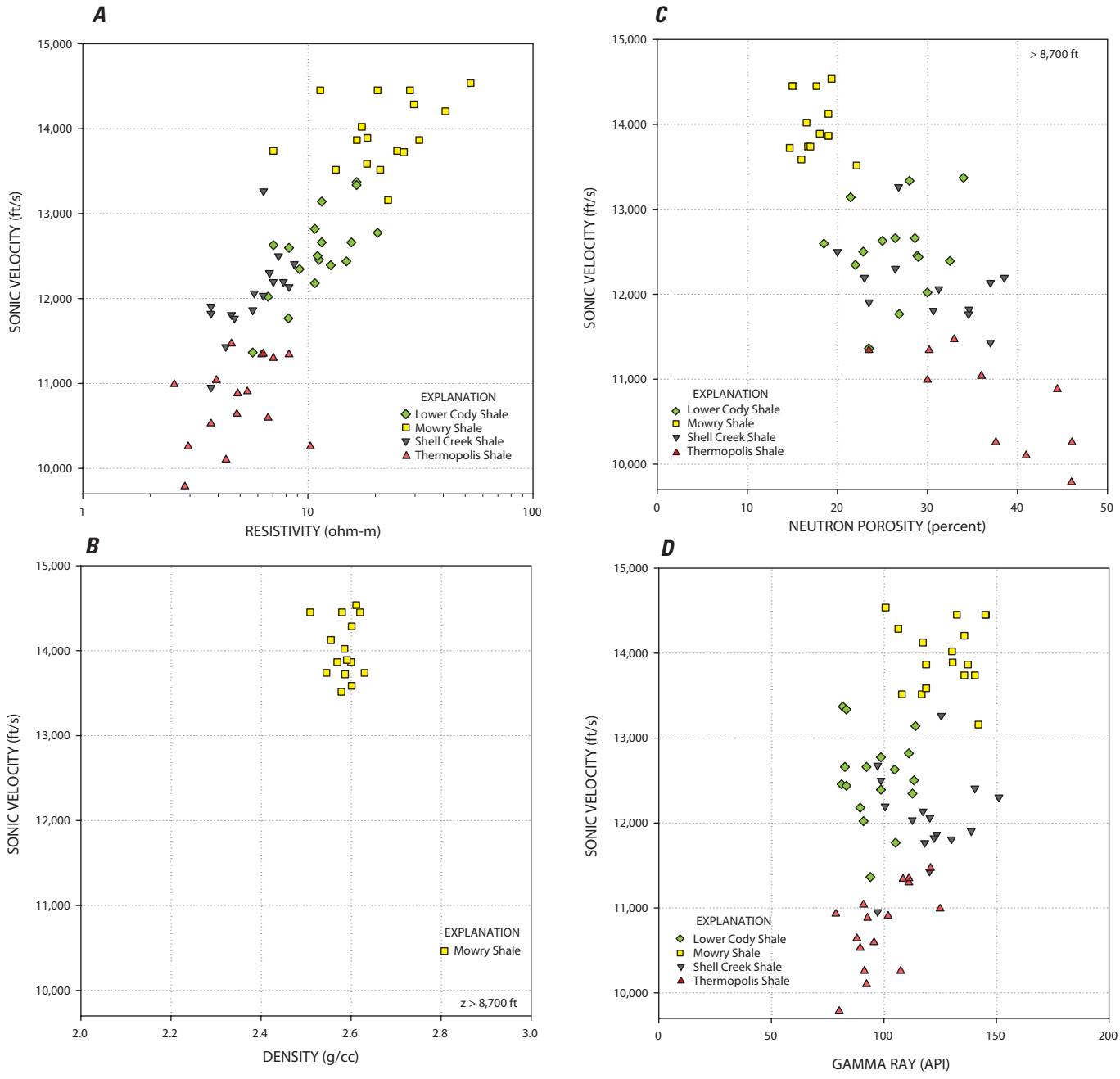

Figure 14. Values of sonic velocity plotted against *A*, resistivity; *B*, density; *C*, neutron porosity; and *D*, gamma-ray activity for four shale units in the Bighorn Basin. All values are determined by an average of a 10 to 20-ft well-log interval in selected shale units. Only values from depths greater than 8,750 ft are shown.

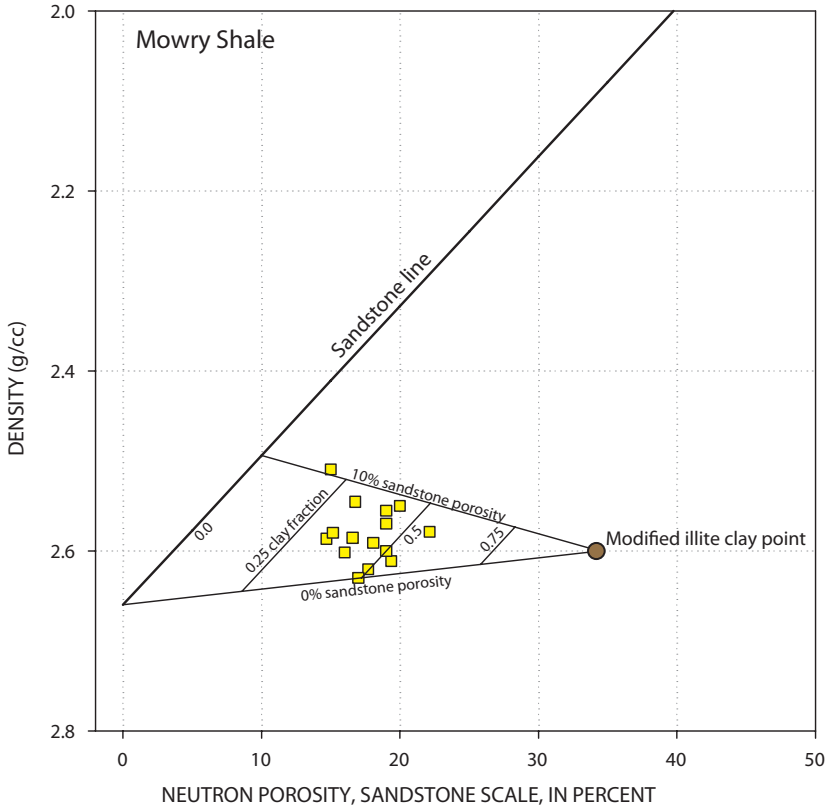

Figure 15. Neutron and density values from the Mowry shale unit. Sandstone line gives porosity-density relation for a sandstone with grain density of 2.66 g/cc. Point labeled illite is selected such that sandstone porosity lines for 0 and 10 percent bracket the data.

1. The range of gamma-ray values (fig. 16) for all four shale units are within the range that is typical of shales. Gamma-ray activity is independent of depth and does not correlate with sonic velocity as do resistivity and neutron response (fig. 14). The level of gamma-ray activity of the Mowry and Shell Creek shale units are similar, and greater than the gamma-ray activity ranges of the lower Cody and Thermopolis shale units (fig. 16*F*).

2. The relatively low neutron porosity and high density of the Mowry shale unit indicates low porosity (five percent or less), high silica content (grain density of 2.66 g/cc), and some illite and kerogen. Based on total organic carbon analyses, kerogen content is around six volume percent. Diagnosis of mineralogical composition from the neutron-density plot (fig. 15) is limited to the Mowry shale unit, the only shale unit for which reliable density data are available. This diagram, an idealization of the true mineralogical composition, indicates a porosity less than 10 percent, and a range of illite content between 30 to 55 percent.

3. The Mowry shale unit is distinguished from the other three shale units by having the highest velocity (fig. 16*B*), the highest resistivity (fig. 16*C*), and the lowest neutron porosity (fig. 16*E*). Although density data could not be reliably obtained from shale units other than the Mowry, it was noted that the density of the Mowry is greater than that of the other three shale units. In addition, a smoother borehole is obtained when drilling the Mowry than in the other three shale units (fig. 16*A*). All of these findings are attributed to the high siliceous content of the Mowry Shale, which has been noted by several authors (tables 2 and 3). High silica (quartz) content must be balanced by low clay content, which is compatible with low neutron response and high resistivity. And high quartz content, along with silica cementation of grains, is compatible with high sonic velocity. However, retention of hydrocarbons

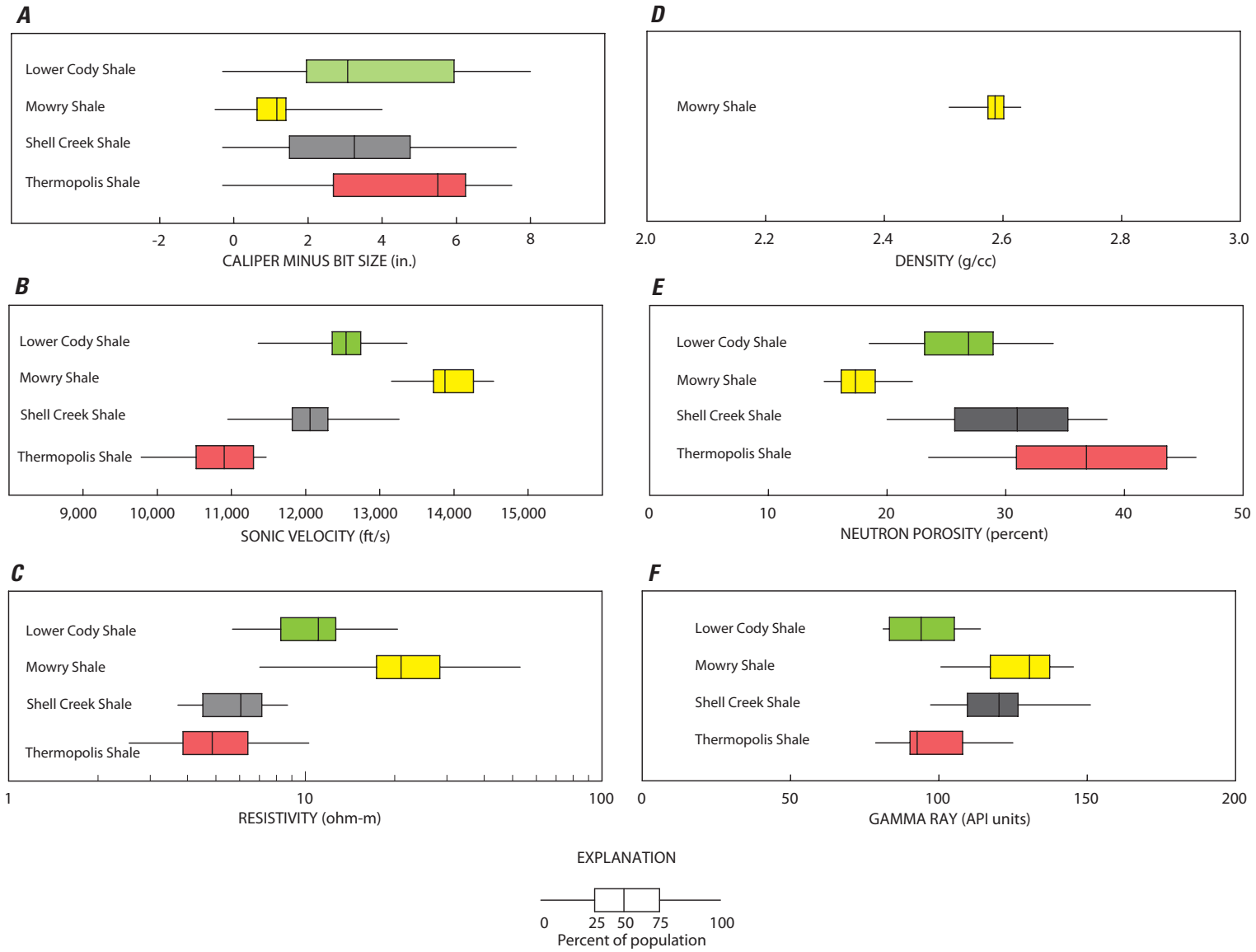

Figure 16. Box-and-whiskers plots of petrophysical properties from well logs, for depths greater than 8,750 ft. Each whisker and each box represents one-fourth of population; vertical line in middle of box represents the median value. *A*, Borehole enlargement as determined by caliper log minus the bit size. *B*, Sonic velocity. *C*, Electrical resistivity. *D*, Density, which is valid only for the Mowry Shale. *E*, Neutron porosity. *F*, Gamma-ray response.

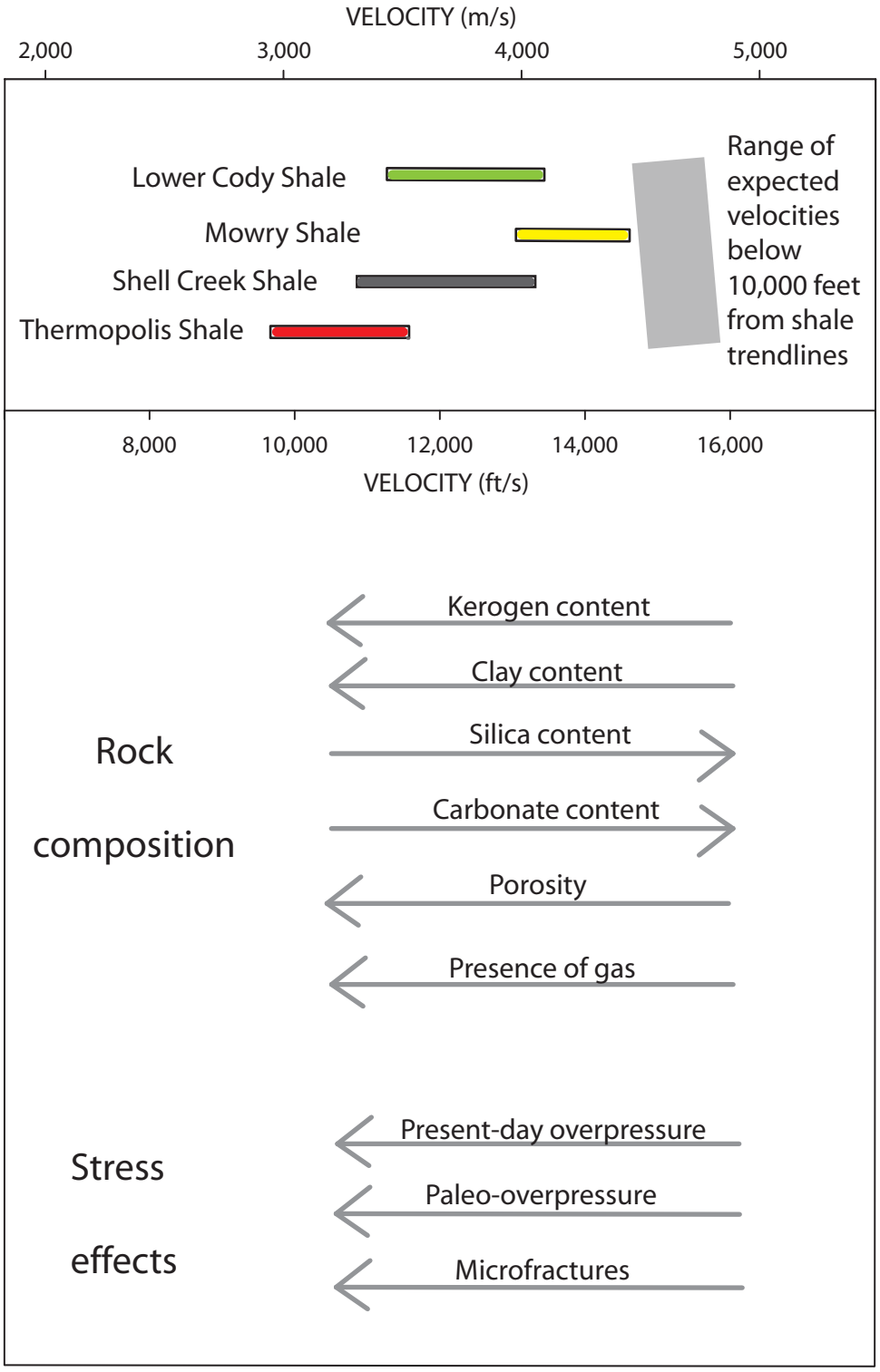

Figure 17. Parameters affecting sonic velocity. Upper part of diagram: range of sonic velocity in four shale units and range of expected velocity in shales from all trendlines below 10,000 ft. Lower part of diagram: nine arrows show consequence of an increase in a given parameter (six related to rock composition and three related to changes in stress) upon sonic velocity. For example, an increase in overpressure is expected to reduce sonic velocity but an increase in silica content is expected to increase sonic velocity.

generated by a good source rock such as the Mowry is not compatible with high velocity, high resistivity, or low neutron porosity. It is possible that low porosity and low compressibility (high modulus) led to the early formation of microfractures so that hydrocarbons were expelled as they were generated, thereby preserving high velocity and high resistivity.

4. Sonic velocity is expected to be affected by clay mineral orientation and location more than it is affected by clay mineralogy. Anisotropy in shales, the change in sonic velocity with direction of propagation, is caused by the presence of flattened grains and microcracks (Vernik and Landis, 1996). Anisotropy affects both sonic velocity and resistivity, which are transport properties, but not neutron and density, which are bulk properties. Laminae and fissility are two macroscopic descriptors related to anisotropy, and neither has been applied to the Mowry Shale, providing another possible explanation for the high velocity and resistivity of the Mowry. One unexplained observation, which is probably related to anisotropy, is the decrease of resistivity with depth below 10,000 ft in all four shale units (fig. 12).

5. The sonic velocity and resistivity of the lower Cody shale unit are less than that of the Mowry shale unit but greater than that of the Shell Creek and Thermopolis shale units (fig. 16). In addition, the neutron porosity of the lower Cody shale unit is less than that of the Shell Creek or Thermopolis shale units. These latter relations are indicative of lower clay content and higher carbonate content in the lower Cody shale unit than in the Shell Creek or Thermopolis shale units. The possibility of high carbonate content rather than high silica content is suggested by the deposition of carbonate-rich sediments in the Niobrara Formation, which is equivalent to the lower Cody Shale, in areas east of the Bighorn Basin (Longman and others, 1998).

6. The Thermopolis Shale is described as a black fissile shale (table 2), and the Thermopolis shale unit has the lowest values of sonic velocity and resistivity (figs. 16*B* and 16*C*) and the highest neutron response (fig. 16*E*). It also tends to create a somewhat larger and rougher borehole than the other shale units (fig. 16*A*). These responses indicate that the Thermopolis shale unit has the highest clay mineral content of the four shale units.

The reductions in sonic velocity and resistivity (fig. 6) and the associated presence of overpressure (fig. 3) highlight an interval that extends from the Cloverly Formation to the base of the Mesaverde Formation (fig. 2). Generation of hydrocarbons, particularly gas, occurred as source rocks were buried to depths of about 15,000 ft (fig. 5). Constrained by the low permeability of fine-grained shales and siltstones, gas could not migrate freely, causing pressure to increase to the point where microfractures were induced, at which point gas could migrate into newly accessible rock volumes. This stepwise migration process of gas generation, pressure increase, fracture opening, and migration continued until gas had migrated into the more accessible units within an interval that extends from the Cloverly Formation upwards into the top of the Cody Shale. The pervasive pressure increase throughout this depth interval caused a drop in effective stress that in turn caused drops in sonic velocity and resistivity. The high pressures that were attained during gas generation at maximum burial have likely decreased with uplift and erosion during the last 10 million years (fig. 4), leaving a record of modest present-day pressures (fig. 3) which are less than maximum paleopressures. As pore pressure builds, the normal increase in effective stress with burial depth is arrested, and the increase in sonic velocity is also arrested or can even decrease if the rocks are unloaded. The reduced values of sonic velocity and resistivity are found in tight sandstone, siltstones, and shales, resulting in the well-log excursions shown in figure 6. Rocks of the Morrison and Cloverly Formations, containing abundant clay minerals of volcanic origin (table 6), form the lower bound of the system. The upper bound of the gas system, located approximately at the top of the Cody Shale, indicates the top of gas migration, which is determined by the amount of gas generated and the concomitant overpressures.

The velocity of shales approaches a limiting value of around 16,000 ft/s at the base of the Cretaceous, as shown by the asymptotic behavior of the lower end of the trendlines (fig. 9*B*), which is established in the "rusty beds" of the Cloverly Formation. The limiting velocity value of each of the four shale units probably differs from that of the "rusty beds," due to variations in the properties of each shale unit, as previously discussed. All four shale units exhibit a marked increase in velocity with depth to a present-day depth of about 10,000 ft, followed by a much smaller rate of increase below that depth (fig. 10), and the density-depth plot for the Mowry shale unit is compatible with the velocity-depth patterns (fig. 13). The separation, or difference, between the velocity in the shale unit and the corresponding trendline velocity does not appear to change much with depth, as demonstrated by plotting the difference in the two velocities as a function of depth (fig. 18). None of the four shale units exhibits any depth dependence in the velocity difference. The compaction process has left an imprint on the velocity of each shale unit, but with an offset that differs for each shale unit, as indicated by the average values posted in figure 18. The true offset for each shale unit is unknown because the true trendline (compaction curve) will differ among the shale units due to variations in mechanical properties. It is proposed in this paper that the sonic velocity has been reduced by overpressure that developed during the course of burial. The steady increase in effective stress that would normally occur with increasing depth of burial was slowed, halted, or even reduced by an increase in pore pressure. As there is no deviation of data shallower than 10,000 ft from the average velocity difference in figure 18, the data suggest that the onset of internal pressure increase occurred at a present-day depth less than 5,000 ft which corresponds to a paleodepth of less than 10,000 ft.

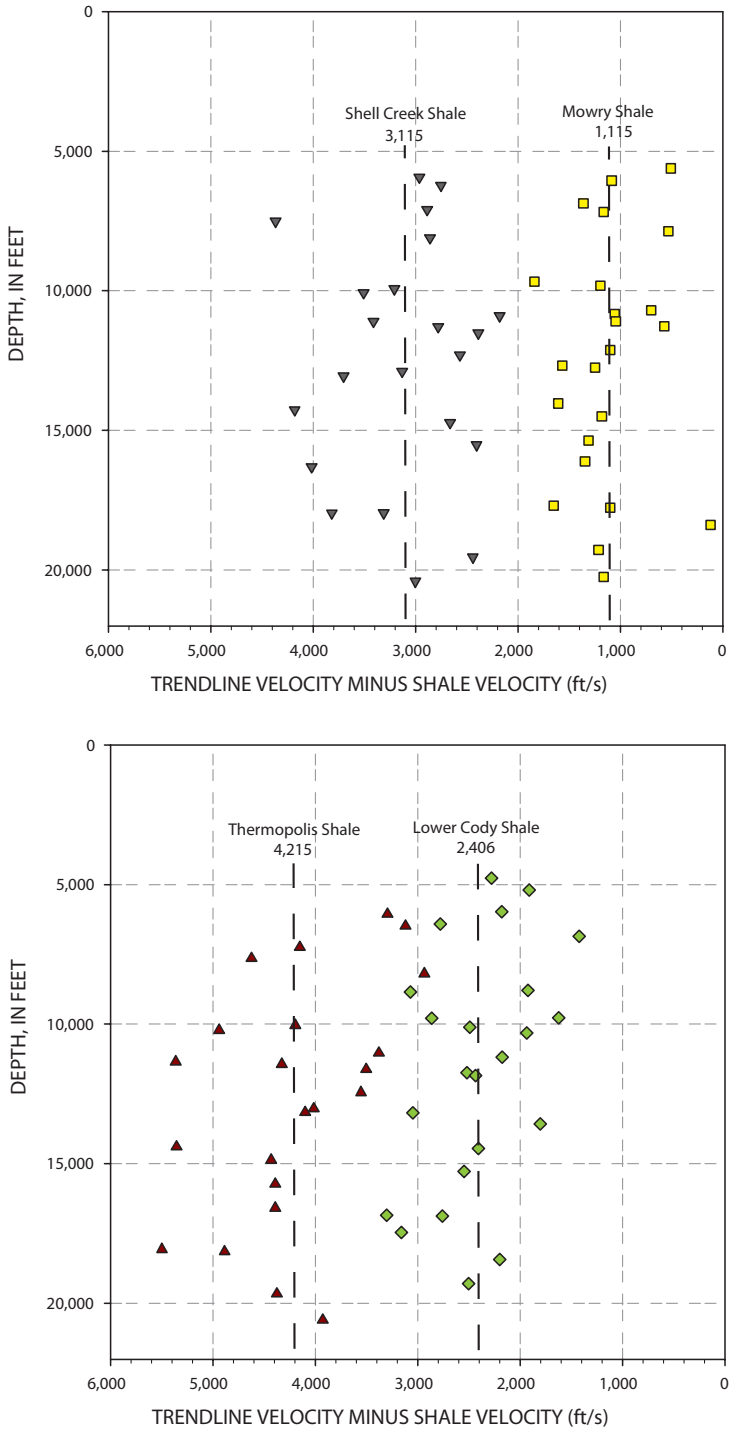

Figure 18. Trendline velocity minus shale unit velocity as a function of depth. Average value for each shale unit is shown as a vertical line. Trendline velocities and shale unit velocities are shown in figure 10. Trendline velocity is selected from the trendline in the same well and at the same depth as the shale unit velocity.

Petroleum generation modeling indicates that gas generation commenced at a burial depth of around 10,000 ft (figs. 4 and 5).

Sonic velocity in the four shale units remains low to the present day, after uplift and possible reduction in pore pressure from maximum pressures reached when strata were more deeply buried. A plausible explanation for the persistence of low sonic velocity is offered in figure 19. The burial history curve for the Thermopolis Shale in the Tatman Mountain Federal well (fig. 4) is reproduced in figure 19*A* with four times at 65, 53, 10, and 0 Ma representing events that impact the evolution of pore pressure and sonic velocity. These four events also appear in figures 19*B*, *C*, and *D*, which display the interdependence of depth, pore pressure, effective stress, sonic velocity, and geologic time. As burial continues and pore pressure builds after time 1, effective stress drops, reaching a minimum at time 3 at the point of deepest burial, where pore pressure reaches 0.9 of lithostatic stress (fig. 19*B*). Sonic velocity follows a loading curve, increasing with burial to time 1 when effective stress stops increasing due to the increase in pore pressure (fig. 19*C*). After time 1, velocity drops, following an unloading curve with a slope that differs markedly from the loading curve. (The loading-unloading scenario is based on the model of Bowers (1994), who noted that rocks do not follow the same stress-strain path for loading and unloading). At time 3 when pore pressure reaches a maxium and effective stress reaches a minimum, sonic velocity also reaches a minimum (fig. 19*C*). With uplift, pore pressure declines from 0.9 to 0.68 of lithostatic stress, effective stress increases correspondingly, and velocity increases to its present-day value at time 4 (figs. 19*B* and *C*). The variation of sonic velocity with depth is plotted in fig. 19*D*. The overall effect of the pore pressure increase is to freeze sonic velocity of the Thermopolis shale unit at a value of around 10,500 ft/s, the observed present-day value in the Tatman Mountain Federal well.

The scenario pictured in figure 19 rests on assumed values of time of commencement of pore pressure increases (time 1), assumed values of pore pressure and effective stress at time 3 and 4, and assumed values defining the loading and unloading curves (fig. 19*C*), although only the initial velocity at zero stress and the slope of the loading curve play a role in the outcome. Other choices for these parameters could easily result in a similar outcome. The main features of the model are the burial history for the Tatman Mountain Federal well (fig. 19*A*), the complementarity of pore pressure and effective stress (fig. 19*B*), and the concept of loading and unloading curves and the cessation of velocity increase (figs. 19*C* and *D*). The result is that a velocity observed in present-day rocks differs little from the velocity obtained at maximum burial. Others have postulated that sonic velocity remains at levels reached during overpressured conditions without undergoing the increases expected due to subsequent drops in pore pressure (Magara, 1978; Cluff and Cluff, 2004).

Summary

Petrophysical properties from well logs have been compiled in 23 wells for four shale units in the Cody, Mowry, Shell Creek, and Thermopolis Shales of the Bighorn Basin. No borehole corrections were applied to any of the measurements, although the need for such corrections was considered before deciding that either corrections were unnecessary or the errors incurred in applying a correction were too great to justify making a correction. Measurements were unavailable for some shale units in some wells due to incomplete penetration of all shale units, incomplete logging runs, poor log quality, or excessive washouts. Statistical summaries of the data are tabulated in Appendix 1 and are shown as summary diagrams in figure 16.

The petrophysical properties of the Mowry Shale are consistent with its overall higher siliceous content relative to the other three shales: sonic velocity is higher, resistivity is higher, and neutron porosity is lower in the Mowry than in the lower Cody, Shell Creek or Thermopolis shale units. The mineral composition of the Mowry Shale appears remarkably similar from well to well within the Bighorn Basin, based upon the tight clustering of the neutron and density well-log responses (figs. 16*D* and 16*E*). In addition, the gamma-ray response of the Mowry is greater than that of the other shale units, although this is not an expected property of highly siliceous rock. Uranium, commonly found in organic matter, or illite, a potassium-bearing clay mineral, could be producing the high gamma-ray response. Illite also has high density and low neutron response and hence its presence is compatible with the density and neutron response of the Mowry Shale (fig.15).

This is not the case however, for the two transport properties: sonic velocity varies as much in the Mowry Shale as in the other three shales and resistivity varies even more (figs. 16*B* and *C*). Moreover, sonic velocity decreases as resistivity decreases—a correlation that is strong when considering all four shale units and weak when considering the Mowry shale unit singly (fig. 14*A*). This correlation between sonic velocity and resistivity can be attributed to the opening of microcracks, causing a slowing of velocity perpendicular to bedding as measured by the sonic velocity log, and a decrease in resistivity parallel to bedding, as measured by the induction log.

All four shale units examined in this study show an increase in sonic velocity to a depth of about 10,000 feet. Below 10,000 ft, there is little or no further change of sonic velocity with depth.

A model combining burial history, the decrease of effective stress with increasing pore pressure, and Bower's model for the dependence of sonic velocity on effective stress has been proposed to explain the persistence of low velocity in shale units. As mentioned in the Introduction, interruptions to compaction gradients associated with gas occurrences and overpressure are observed in correlative strata in other basins in Wyoming, so the general results for shales in the Bighorn Basin established in this paper should be applicable elsewhere.

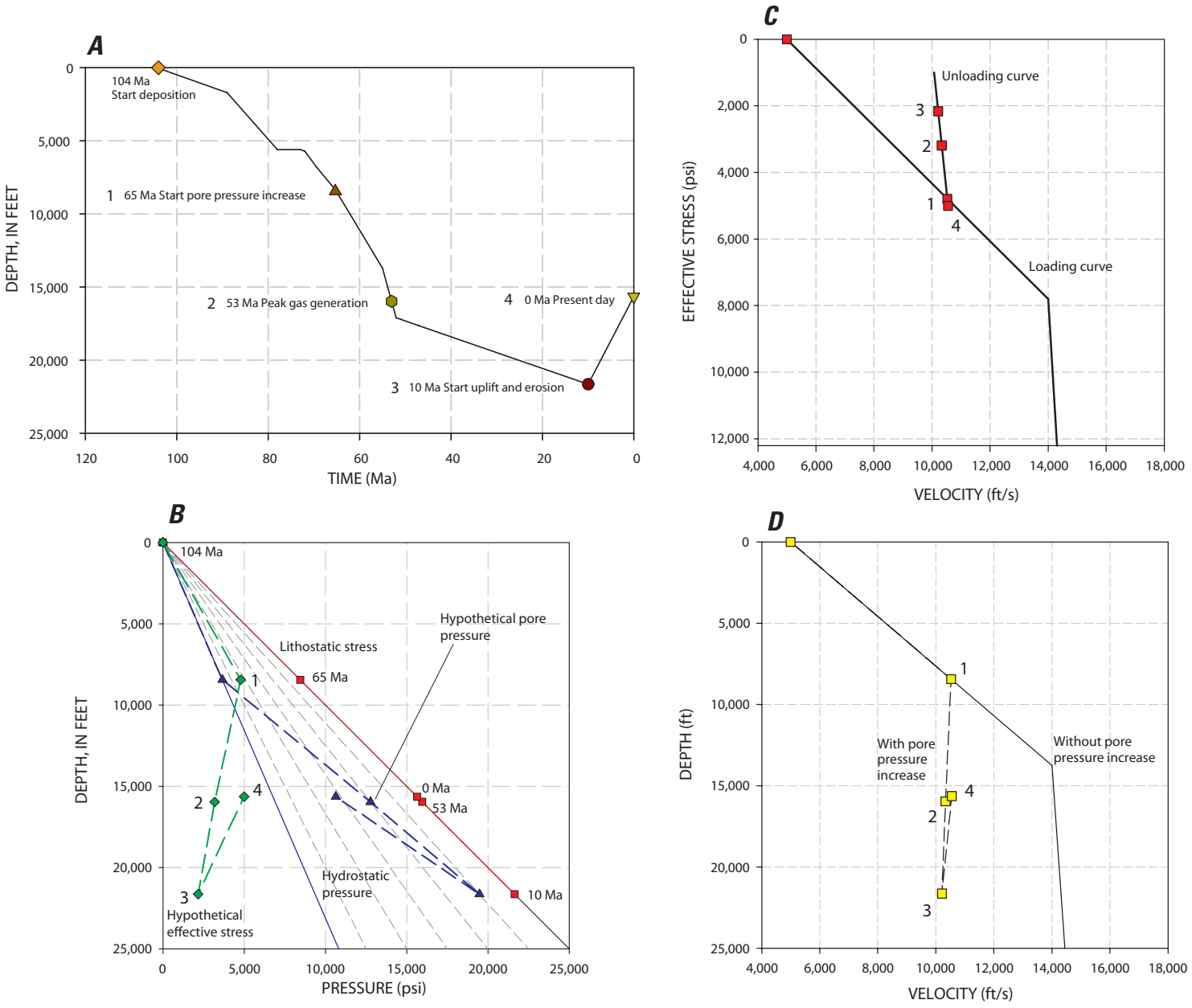

Figure 19. Evolution of pore pressure, effective stress, and sonic velocity at four times in the Thermopolis shale unit, Tatman Mountain Federal well. *A*, Burial history from Roberts and others (2008) with times of four events. *B*, Pore pressure and effective stress as function of depth. *C*, Sonic velocity as a function of effective stress. *D*, Sonic velocity as a function of depth.

Acknowledgments

During the course of this investigation, useful discussions were held with Tom Finn, Mark Kirschbaum, Neil Fishman, Paul Lillis, and Chris Schenk of the U.S. Geological Survey, and Mike Batzle and Manika Prasad of the Colorado School of Mines. Reviews by Tom Finn, Lori Burke, and Neil Fishman led to improvements in the manuscript.

References Cited

Baker, L.J., 1984, The effect of the invaded zone on full wave-train acoustic logging: Geophysics, v. 49, no. 6, p. 769–809.

Bowers, G.L., 1994, Pore pressure estimation from velocity data: Accounting for overpressure mechanisms besides undercompaction: IADC/Society of Petroleum Engineers Drilling Conference, paper 27488, p. 515–530.

Bredehoeft, J.D., Belitz, K., and Sharp-Hansen, S., 1992, The hydrodynamics of the Big Horn Basin: A study of the role of faults: American Association of Petroleum Geologists Bulletin, v. 76, no. 4, p. 530–546.

Cluff, R.M., and Cluff, S.G., 2004, The origin of Jonah field, northern Green River basin, Wyoming, Chapter 8 *in* Robinson, J.W., and Shanley, K.W., eds., Jonah Field: case study of a tight-gas fluvial reservoir: American Association of Petroleum Geologists Studies in Geology 52 and Rocky Mountain Association of Geologists 2004 Guidebook, p. 127–145.

Davis, J.C., 1967, Petrology of the Mowry Shale: University of Wyoming, Ph.D. Thesis, 141 p.

Davis, J.C., 1970, Petrology of Cretaceous Mowry Shale of Wyoming: American Association of Petroleum Geologists Bulletin, v. 54, no. 3, p. 487–502.

Eicher, D.L., 1962, Biostratigraphy of the Thermopolis, Muddy, and Shell Creek Formations, *in* Enyert, R.L., and Curry, W.H., III, eds., Symposium on Early Cretaceous rocks of Wyoming and adjacent areas, 17th Annual Field Conference: Wyoming Geological Association Guidebook, p. 72–93.

Ellis, D.V., and Singer, J.M., 2008, Well logging for earth scientists: Springer, The Netherlands, 692 p.

Ferrell, R.E., Jr., 1965, Paleoenvironmental significance of clay minerals in the Shell Creek Shale, Muddy Sandstone, and Thermopolis Shale on the east flank of the Bighorn Mountains, Wyoming: University of Illinois, unpub. M.S. thesis, 67 p.

Gutierrez, M.A., Couzens, B.A., and Braunsdorf, N.R., 2006, Evaluation of sonic velocity anomalies associated with basin-centered gas accumulations in the Greater Green River Basin, Wyoming: Abstract for AAPG annual meeting, Houston, Texas: American Association of Petroleum Geologists Bulletin, v. 90.

Hearst, J.R, Nelson, P.H., and Paillett, F.L., 2000, Well logging for physical properties: John Wiley & Sons, Ltd., London, 483 p.

IHS Energy, 2007, U.S. Production and Well Data: Englewood, Colo., database available from IHS Energy, 15 Inverness Way East, D205, Englewood, CO 80112, U.S.A.

Japsen, P., Muderji, T., and Mavko, G., 2007, Constraints on velocity-depth trends from rock physics models: Geophysical Prospecting, v. 55, p. 135–154.

Johnson, R.C., and Finn, T.M., 1998, Is there a basin-centered gas accumulation in Upper Cretaceous rocks in the Bighorn Basin?, *in* Keefer, W.R., and Goolsby, J.E., eds., Cretaceous and Lower Tertiary rocks of the Bighorn Basin, Wyoming and Montana: Wyoming Geological Association 49th Guidebook, p. 257–273.

Katahara, K., 2008, What is shale to a petrophysicist?: The Leading Edge, v. 27, no. 6, p. 738–741.

Keefer, W.R., Finn, T.M., Johnson, R.C., and Keighin, C.W., 1998, Regional stratigraphy and correlation of Cretaceous and Paleocene rocks, Bighorn Basin, Wyoming and Montana, *in* Keefer, W.R., and Goolsby, J.E., eds., Cretaceous and Lower Tertiary rocks of the Bighorn Basin, Wyoming and Montana: Wyoming Geological Association 49th Guidebook, p. 1–30.

Longman, M.W., Luneau, B.A., and Landon, S.M., 1998, Nature and distribution of Niobrara lithologies in the Cretaceous Western Interior Seaway of the Rocky Mountain Region: The Mountain Geologist, v. 35, no. 4, p. 137–170.

MacQuaker, J.H.S., and Jones, C.R., 2002, A sequence-stratigraphic study of mudstone heterogeneity: A combined petrographic/wireline log investigation of Upper Jurassic mudstones from the North Sea (U.K.), *in* Lovell, M. and Parkinson, N., eds., Geological applications of well logs: American Association of Petroleum Geologists Methods in Exploration no. 13, p. 123–141.

Magara, K., 1978, Compaction and fluid migration: Practical petroleum geology: Elsevier Scientific Publishing Co., New York, 319 p.

Moberly, R., Jr., 1960, Morrison, Cloverly, and Sykes Mountain Formations, northern Bighorn Basin, Wyoming and Montana: Bulletin of Geological Society of America, v. 71, p. 1137–1176.

Moberly, R., Jr., 1962, Lower Cretaceous history of the Bighorn basin, Wyoming, *in* Symposium on Early Cretaceous rocks of Wyoming and adjacent areas, Enyert, R.L., and Curry, W.H., III eds., 17th Annual Field Conference: Wyoming Geological Association Guidebook, p. 94–101.

Pettijohn, F.J., 1975, Sedimentary rocks: Harper & Row, New York, 628 p.

Roberts, L.N.R., Finn, T.M., Lewan, M.D., and Kirschbaum, M.A., 2008, Burial history, thermal maturity, and oil and gas generation history of source rocks in the Bighorn Basin, Wyoming and Montana: U.S. Geological Survey Scientific Investigations Report 2008–5037, 28 p.

Schlumberger, 1996, Log interpretation charts: Schlumberger Wireline and Testing, Houston, Texas, 188 p.

Surdam, R.C., Jiao, Z.S., and Heasler, H.P., 1997, Anomalously pressured gas compartments in Cretaceous rocks of the Laramide basins of Wyoming: A new class of hydrocarbon accumulation, *in* Surdam, R.C., ed., Seals, traps, and the petroleum system: American Association of Petroleum Geologists Memoir 67, p. 199–222.

Vernik, L., 1997, Predicting porosity from acoustic velocities in siliciclastics: a new look: Geophysics, v. 62, no. 1, p. 118–128.

Vernik, L., and Landis, C., 1996, Elastic anisotropy of source rocks: implications for hydrocarbon generation and primary migration: American Association of Petroleum Geologists Bulletin, v. 80, no. 4, p. 531–544.

Appendix 1

Appendix 1. File containing petrophysical responses in four shale units in 23 wells.

Well Information

Map Number	Lease Name	Well Number	Bit Size (in.)	Type fluid in well	Mud weight (lb/gal)
15	Buffalo Creek	1	8.75	Fresh gel mud	8.9
13	Bar TL	2	7.875	Chem-Gel	9.5
20	Gywnn Ranch	1	7.875	Oil emulsion	9.4
1	State	56-16	8.75	Gel Chem	8.8
18	Worland Unit	47T-M28	7.875	Chem-Gel	9.3
21	Blue Mesa	1-30	7.875	Fresh gel mud	9.1
3	Gulch	1	8.75	Fresh gel mud	9.3
23	Federal	1-2	8.75	Gel Chem	9.2
4	Spear-Federal	33-31	8.75	Fresh gel mud	10.2
10	Adams	1	8.75	Chem-Gel	9.1
22	Federal 15-22	1	7.875	Chem Gel	9.1
12	Predicament	1-31-3D	8.75	KCl mud	8.9?
11	Fritz-Federal	1-16 2B	8.75	KCl-Dispac	9.1
2	McCullough II	3-27	8.5	KCl mud	9.6
9	Michaels Ranch	17-15	8.5	Fresh gel mud	9.2
19	Gillies Draw Unit	1	8.5	Fresh gel mud	9.4
14	Tatman Mtn Federal	1-20	8.5	Dispersed	9.04
5	Bridger Trail Unit	2-A	8.5	KCl mud	9
8	Emblem Bench	1	7.875	KCl mud	10.7
17	Ridge Unit	1-21	8.5	Fresh gel mud	9.2
6	Red Point II Unit	1	6	Fresh gel mud	10.1
16	Sellers Draw Unit	1	8.75	Fresh gel mud	9.3
7	Katrine Loch	1	8.9	Oil base mud	11.0?

11/24/2009	Statistical summary for all 23 wells
	Statistical summary for depths greater than 8,750 ft

Appendix 1. File containing petrophysical responses in four shale units in 23 wells.—Continued

Lower Cody Shale									
Depth (ft)	Vtrendline (ft/s)	Vshale unit (ft/)	Vdifference (ft/s)	Neutron (percent)	Density (g/cc)	Resistivity (ohm-m)	Gamma ray (API)	Caliper (in.)	Caliper-Bit (in.)
4771	13388	11111	2277			4.3	114.2	11.7	3.0
5203	12781	10870	1911			3.9	109.6	9.0	1.1
5968	13291	11111	2180			6.3	103.4	9.4	1.5
6418	14489	11710	2780	28.0		6.3	89.6	15.0	6.3
6861	12582	11161	1421			9.2	118.8	10.5	2.6
8792	14745	12821	1924			10.8	111.1	9.0	1.1
8849	15250	12180	3069			10.8	89.6	15.4	6.7
9779	14078	12453	1625	28.9		11.2	81.2	10.6	1.9
9792	15522	12658	2864	28.6		15.6	82.8	12.0	3.3
10114	14883	12392	2491	32.5		12.6	98.8	11.5	2.8
10321	14704	12771	1932			20.4	98.8	9.8	1.9
11184	14674	12500	2174	22.9		11.0	113.3	14.5	5.8
11744	15113	12594	2519	18.5		8.3		10.7	2.0
11848	15062	12626	2436	25.0		7.0	104.9	11.3	2.8
13176	15065	12019	3046	30.0		6.7	91.0	14.2	5.7
13572	15169	13369	1800	34.0			81.8	14.5	6.0
14451	14846	12438	2408	29.0		14.8	83.3	12.8	4.3
15280	15687	13141	2546	21.5		11.5	114.0	10.5	2.0
16851	15068	11765	3303	26.9		8.2	105.2	14.5	6.6
16871	15418	12658	2760	26.4		11.5	92.3	16.5	8.0
17467	14522	11364	3158	23.5		5.7	94.1	8.9	2.9
18428	15534	13333	2201	28.0		16.5	83.3	16.1	7.4
19296	14848	12346	2503	22.0	2.64	9.2	112.7	8.6	-0.3
Minimum		10870	1421	18.5		3.9	81.2	8.9	1.1
Maximum		13369	3303	34.0		20.4	118.8	16.5	8.0
Average		12234	2406	26.6		10.1	98.8	12.2	3.9
Count		23	23	16		22	22	22	22
Standard deviation		727	503	4.2		4.2	12.5	2.5	2.2
Minimum		11364		18.5		5.7	81.2		-0.3
25th percentile		12357		23.2		8.3	83.3		2.0
Median		12547		26.9		11.0	94.1		3.1
75th percentile		12743		28.9		12.6	105.2		5.9
Maxiumum		13369		34.0		20.4	114.0		8.0

Appendix 1. File containing petrophysical responses in four shale units in 23 wells.—Continued

Mowry Shale

Depth (ft)	Vtrendline (ft/s)	Vshale unit (ft/)	Vdifference (ft/s)	Neutron (percent)	Density (g/cc)	Resistivity (ohm-m)	Gamma ray (API)	Caliper (in.)	Caliper-Bit (in.)
5617	13461	12953	508		2.52	9.2	151.2	9.5	0.8
6057	13103	12019	1084		2.39	6.3	137.3	8.6	0.7
6871	13773	12413	1360			12.6	121.9	8.6	0.7
7175	14721	13557	1164	20.0	2.55	10.8	125.0	10.3	1.6
7871	12846	12315	530		2.51	7.8	132.7	8.7	0.8
9674	14995	13158	1837			22.7	142.0	8.5	0.6
9824	15481	14286	1195		2.60	29.6	106.4	10.2	1.5
10702	14212	13514	698	22.1	2.58	21.0	116.9	10.6	1.9
10835	15588	14535	1053	19.4	2.61	52.9	100.8	10.0	1.3
11100	14911	13866	1045	19.0	2.57	31.3	137.3	10.0	1.3
11273	14775	14205	571			40.9	135.8	9.0	1.1
12123	14834	13736	1098	16.8	2.55	24.9	140.4	9.5	0.8
12682	15287	13721	1566	14.7	2.59	26.7		10.0	1.3
12751	15113	13866	1247	19.0	2.60	16.5	118.8	9.7	1.2
14033	15118	13514	1604			13.3	108.0	12.5	4.0
14497	15305	14124	1180	19.0	2.56		117.3	10.5	2.0
15364	14896	13587	1309	16.0	2.60	18.3	118.8	9.5	1.0
16111	15796	14451	1345	15.2	2.58	20.4	145.3	9.1	0.6
17769	15120	14021	1098	16.6	2.59	17.4	130.3	8.5	0.6
17691	15541	13889	1652	18.1	2.59	18.4	130.6	10.0	1.5
18379	14570	14451	119	15.0	2.51	11.4	145.1	5.5	-0.5
19282	15664	14451	1213	17.7	2.62	28.4	132.4	9.3	0.6
20246	14898	13736	1161	17.0	2.63	7.0	135.8	9.0	0.1
Minimum		12019	119	14.7	2.39	6.3	100.8	5.5	-0.5
Maximum		14535	1837	22.1	2.63	52.9	151.2	12.5	4.0
Average		13668	1115	17.7	2.56	20.4	128.6	9.5	1.1
Count		23	23	15	19	22	22	22	22
Standard deviation		697	406	2.1	0.06	11.5	13.6	1.3	0.8
Minimum		13158		14.7	2.51	7.0	100.8		-0.5
25th percentile		13725		16.1	2.57	17.4	117.3		0.6
Median		13877		17.3	2.59	21.0	130.6		1.2
75th percentile		14265		19.0	2.60	28.4	137.3		1.4
Maxiumum		14535		22.1	2.63	52.9	145.3		4.0

Appendix 1. File containing petrophysical responses in four shale units in 23 wells.—Continued

Shell Creek Shale									
Depth (ft)	Vtrendline (ft/s)	Vshale unit (ft/)	Vdifference (ft/s)	Neutron (percent)	Density (g/cc)	Resistivity (ohm-m)	Gamma ray (API)	Caliper (in.)	Caliper-Bit (in.)
5939	13489	10526	2963			2.8	134.2	11.5	2.8
6227	13169	10417	2753			2.6	137.3	9.0	1.1
7097	13900	11013	2886			4.3	101.9	9.0	1.1
7508	14826	10460	4365			3.5	121.9	13.0	4.3
8106	12909	10050	2858			4.3	111.1	14.5	6.6
9931	15070	11862	3207			5.7	123.4	8.7	0.8
10069	15540	12034	3507			6.3	112.7	12.0	3.3
10900	14241	12063	2178	31.3		5.8	120.4	13.5	4.8
11099	15605	12195	3410	38.6		7.8	100.6	13.5	4.8
11290	14916	12136	2780	37.0		8.3	117.3	12.5	3.8
11517	14794	12407	2387			8.7	140.4	9.5	1.6
12302	14865	12300	2565	26.4		6.8	151.1	10.5	1.8
12891	15327	12195	3132	23.0		7.0		9.7	0.9
13052	15130	11429	3702	37.0		4.3	120.3	14.0	5.5
14268	15133	10953	4180			3.7	97.2	14.5	6.0
14720	15338	12674	2664				97.2	16.1	7.6
15518	14905	12500	2405	20.0		7.4	98.8	11.5	3.0
16303	15821	11806	4015	30.7		4.6	130.0	10.0	1.5
17954	15130	11820	3310	34.6		3.7	122.3	12.5	4.6
17957	15581	11765	3817	34.6		4.7	118.2	15.0	6.5
Not reached									
19536	15703	13263	2440	26.8		6.4	125.6	9.5	0.8
20399	14906	11905	3001	23.5	2.67	3.7	138.9	8.6	-0.3
Minimum		10050	2178	20.0		2.6	97.2	8.7	0.8
Maximum		13263	4365	38.6		8.7	151.1	16.1	7.6
Average		11717	3115	30.3		5.4	120.0	11.9	3.5
Count		22	22	12		21	21	21	21
Standard deviation		825	613	6.2		1.8	15.4	2.3	2.2
Minimum		10953		20.0		3.7	97.2		-0.3
25th percentile		11820		25.7		4.5	109.6		1.5
Median		12063		31.0		6.1	120.4		3.3
75th percentile		12300		35.2		7.1	126.7		4.8
Maxiumum		13263		38.6		8.7	151.1		7.6

Appendix 1. File containing petrophysical responses in four shale units in 23 wells.—Continued

Thermopolis Shale									
Depth (ft)	Vtrendline (ft/s)	Vshale unit (ft/)	Vdifference (ft/s)	Neutron (percent)	Density (g/cc)	Resistivity (ohm-m)	Gamma ray (API)	Caliper (in.)	Caliper-Bit (in.)
6060	13500	10204	3295			3.0	106.4	13.0	4.3
6484	13271	10152	3118			3.5	108.0	11.0	3.1
7243	13982	9833	4149			4.6	75.7	12.0	4.1
7645	14869	10246	4623	47.0		3.2	100.3	18.0	9.3
8197	12933	10000	2933			4.6	91.0	14.0	6.1
10037	15101	10905	4196			5.4	101.9	9.5	1.6
10216	15576	10638	4938			4.8	88.0	16.0	7.3
11031	14260	10881	3379	44.4		4.9	92.8	12.0	3.3
11344	15620	10256	5364	46.1		10.3	91.3	12.5	3.8
11438	14920	10593	4327			6.7	95.7	15.0	6.3
11618	14801	11299	3502			7.0	111.1	10.0	2.1
12447	14890	11338	3552	30.2		6.2	108.6	15.0	6.3
13024	15352	11338	4014	23.5		8.3		10.5	1.8
13160	15136	11038	4099	36.0		3.9	91.0	15.0	6.5
14390	15140	9785	5355	46.0		2.8	80.2		
14867	15360	10929	4431				78.7	>16	
15724	14916	10526	4390			3.7	89.6	14.0	5.5
16580	15858	11468	4390	33.0		4.6	120.8	14.0	5.5
18148	15141	10256	4885	37.6		2.9	107.6	14.0	6.1
18064	15598	10101	5497	41.0		4.3	92.3	16.0	7.5
Not reached									
19656	15721	11348	4373			6.3		15.0	6.3
20594	14916	10989	3927	30.0	2.65	2.6	125.0	8.6	-0.3
Minimum		9785	2933	23.5		2.6	75.7	9.5	1.6
Maximum		11468	5497	47.0		10.3	125.0	18.0	9.3
Average		10642	4215	37.7		4.9	97.8	13.5	5.1
Count		22	22	11		21	20	19	19
Standard deviation		537	725	7.9		2.0	13.3	2.3	2.1
Minimum		9785		23.5		2.6	78.7		-0.3
25th percentile		10526		30.9		3.9	90.3		2.7
Median		10905		36.8		4.9	92.8		5.5
75th percentile		11299		43.6		6.4	108.1		6.3
Maxiumum		11468		46.1		10.3	125.0		7.5

Click here to return to
Volume Title Page